Role of Nucleon-Exchange in the Breakup of Deuterons by Incident Protons at Low Energy

BY

Abed Ahmad Moussa

A Thesis

Submitted to the Faculty of Graduate Studies
in partial fulfillment of the requirements
for the degree of
Master of Science

in

Department of Physics
University of Manitoba
Winnipeg, Manitoba

ISBN 0-315-37322-9

ROLE OF NUCLEON-EXCHANGE IN THE BREAKUP OF DEUTERONS BY INCIDENT PROTONS AT LOW ENERGY

BY

ABED AHMAD MOUSSA

A thesis submitted to the Faculty of Graduate Studies of the University of Manitoba in partial fulfillment of the requirements of the degree of

MASTER OF SCIENCE

ACKNOWLEDGEMENTS

The author wishes to express his deepest gratitude to his supervisor Professor J.S.C. McKee, for his continuous help and encouragement, as well as very many valuable suggestions during the completion of this work.

It is a great pleasure to thank Dr. Jim Birchall who has been involved at every stage of this project and contributed a great deal of advice and practical help.

Thanks are also due to members of the cyclotron laboratory staff and Mechanical and Electrical workshop personnel of the Department of Physics for their advice and help during various stages of work.

Thanks are also due to all the people who collaborated and helped on this project.

Thanks are also due to Kelly Harris for assisting in the preparation of this thesis.

Financial support from the Natural Sciences and Engineering Research Council of Canada and the University of Manitoba made it possible for the author to undertake this program of study.

ABSTRACT

As discussed by Shapiro([1],[2]), the Treiman-Yang criterion can be used to identify nucleon exchange as the dominant mechanism by which the deuteron breakup reaction $^2H(p,2p)n$ proceeds at 11.2 MeV incident energy.

Proton deuteron coincidence spectra were obtained for seven different values of the Treiman-Yang angle ε. Results indicate that nucleon exchange is not a completely dominant process for the condition studied because of large momentum transfer. In this experiment one proton counter (θ_1,Φ_1) (with respect to the beam) was maintained in a fixed position of $\theta_1 = 15°$, and a second proton counter (θ_2,Φ_2) was rotated around the direction of nucleon transfer on a cone of 20° opening angle.

For completeness, the results of this experiment are compared with the predictions of exact calculations by J.P. Svenne using the Dolechall code([27]). Comments on this comparison are given in the conclusion.

TABLE OF CONTENTS

THE $^{2}H(p,2p)n$ Reaction

CHAPTER ONE

INTRODUCTION

1.1 FEATURES OF THE THREE-BODY BREAKUP REACTION

The description of nuclear reactions, which are in fact many-body processes, is usually reduced to a two- or a three-body problem which is solved by the use of more or less phenomenological models. Many such models have been used to describe direct reactions (plane-wave impulse and distorted-wave Born approximations, etc). Another approach suggested by Shapiro([1]) is to apply to direct nuclear reactions the Feynman-graph technique, previously developed for elementary particle physics. In using this method there is, in general, no simple way to select the particular graphs which are dominant for a given reaction mechanism. Such a selection can only be made by the study of the proximity of the graphs' singularities. However, this requires the consideration of all possible graphs.

In the case of knock-out reactions, the structure of the scattering amplitude corresponding to the pole graph in the Feynman series, provided the matrix element can be factorized, is particularly simple and has experimentally observable consequences.

For deuteron breakup by protons and similar processes, provided the exchanged particle has spin 0 or ½([2]), the amplitude is invariant under rotation of the reaction plane around the transferred momentum in the proton rest frame. This invariance([3]) which was already pointed out in the case of

deuteron stripping([4]) is a necessary but not a sufficient condition for the dominance of the pole graph. As pointed out by Kolybasov([5]), under certain conditions and approximations some triangular graphs (such as graphs corresponding to spinless particles and constant vertices) may satisfy this condition.

However, a Treiman-Yang test provides a strong indicator for the pole-graph description of the reaction mechanism.

Measurements of deuteron breakup reactions have shown cross-section enhancements in two kinematical regions, one corresponding to a low relative energy of a pair of nucleons (final-state interaction), the other to a small momentum transfer to one nucleon. This second enhancement, corresponding to the quasi-free kinematical condition, is usually described by the impulse approximation([6],[7]).

In the Feynman-graph formalism, the pole graph also predicts an enhancement at low momentum transfer. However, the existence of such an enhancement in the experimental data does not necessarily imply that this graph represents a dominant contribution([8]).

Therefore, in a three-body break up reaction which yields three particles in the final state, there are a number of physical processes which can occur before the particles assume their asymptotic momentum and energy values. These reactions may cause enhancements in the energy spectra of the particles. Examples of these processes are shown in figure (1.1) where b refers to a single bombarding particle incident on two bound particles t.

Diagram (a) of figure (1.1) is a direct breakup reaction, also known as the 'background' contribution process. This process produces a smooth momentum or energy distribution (provided that the transition matrix element does not exhibit any strong fluctuations) whose shape is governed by phase space considerations.

Diagrams (b) to (d) cause deviations away from the pure differential phase space distribution, characterized in general by peaks in the energy spectra. Depending on the reaction kinematics, coulomb interactions can modify the differential phase space distributions. Diagram (b) is a quasi-free scattering (QFS) process. Here the incident particle is regarded as having scattered from one of the constituent particles of the target nucleus with the other target particle left undisturbed. In the case of an S-wave distribution of the target constituents, this gives rise to a peak in the energy spectra in a region where the spectator particle has near zero momentum.

Diagram (c) is a pictorial representation of a final state interaction (FSI) process. Here break up of the target nucleus is followed by strong interaction between particles (3) and (4). It is assumed that the (3,4) subsystem has relatively little interaction with particle (5). Consequently particle (5) and the interaction volume of particles (3,4) must separate rapidly. In nucleon-nucleon (NN) interactions, FSI are characterized by near zero relative momentum between the two nucleons (3) and (4). The triangle graph, diagram (d), represents the first of an infinite series of correction terms to the scattering process. The process denoted by diagram (d) can be directly measured provided the following kinematical conditions

hold([47]). The two nucleons (3,4) will initially be emitted, in the overall centre of mass system, in a direction antiparallel to (5'). The composite particle then decays emitting particle (4') in a direction parallel to (5') but with a greater velocity. This results in the two particles (4') and (5') undergoing a rescattering process called proximity scattering.([48])

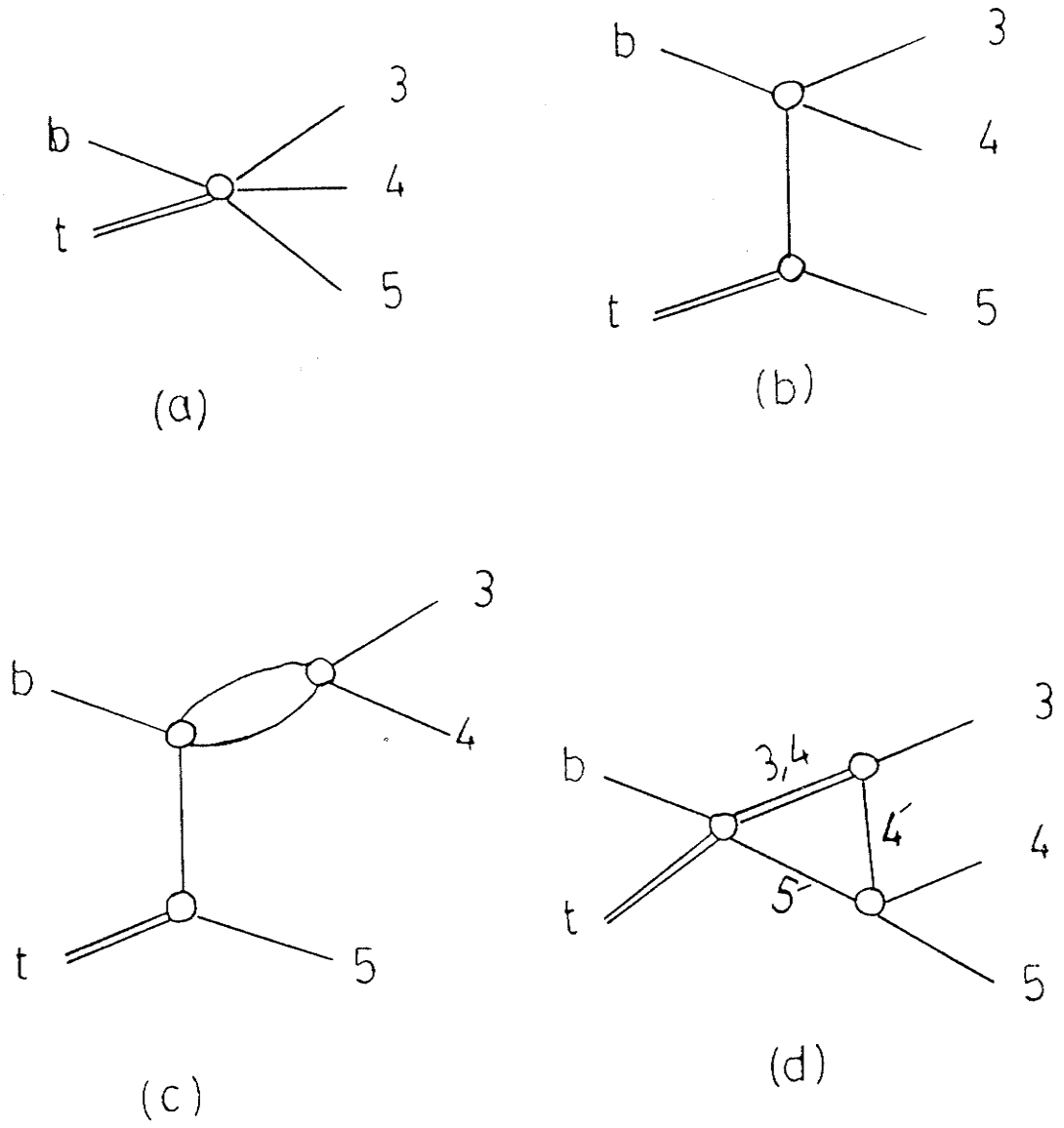

fig (1.1) Feynman diagrams for possible processes resulting in three particles in the final state from the reaction b+t ---> 3+4+5

(a) direct breakup
(b) quasi-free scattering
(d) final state interaction
(e) sequential decay followed by rescattering

1.2 MOTIVATION FOR PRESENT EXPERIMENT

In this work, the three-body reaction selected was the breakup of deuterons induced by 11.2 MeV protons. Experimental few-nucleon studies on deuteron break up reactions have unambiguously shown that, apart from local enhancements due to final-state interactions (FSI), the differential cross-section is largely characterized by quasi-free scattering behaviour. The characteristic peaking at low-momentum transfers even persists down to such low energies that pure QFS hardly can occur. It is therefore relevant to investigate whether observed QFS phenomena are actually consistent with the idea of a true spectator, i.e., that they arise from a simple pole graph. In that case, as shown by Treiman and Yang([3]) for charged pion exchange not using any additional ad hoc assumption, the pole-graph amplitude should be invariant with respect to rotations around the momentum-transfer vector for the transferred particle in the rest frame of the quasi-elastically scattered initial particle. The Treiman-Yang test (TY) has rarely been applied to nucleon or charge exchange processes([9],[10],[11]).

The purpose of the present experiment is to study the importance of the pole graph in the low-energy deuteron breakup by performing the Treiman-Yang test.

In the next chapter a discussion is given for three-nucleon kinematics, three body breakup calculations and the Treiman-Yang criterion in deuteron breakup is also presented.

In chapter three a review of previous work on deuteron breakup is presented. References to the literature are given where full details of calculations are available.

Details of the experimental equipment, electronics and the data collection procedure and software are given in chapter four. An analysis of the data, their reliability and conclusions are drawn from this research.

CHAPTER TWO

THEORY

2.1 KINEMATICS OF SYSTEMS WITH THREE NUCLEONS IN THE FINAL STATE

The notation adopted is shown in fig (2.1) where the Z axis is defined to be parallel to the incident beam direction. The detected particles in this notation are 3 and 4, both protons in the present experiment, a study of the $^2H(p,2p)n$ reaction. The undetected neutron is labeled 5. As the plane of scattering for the third particle was not changed, the detector to the right of the incident beam axis is referred to as the 'in-plane' counter telescope. The second counter telescope, for which the azimuthal angle ϕ_4 was in general not equal to zero or 180 degrees is called the 'out-of-plane' counter telescope.([14])

For a particle of rest mass m_0 the following relationship holds

$$E^2 = (P\ C)^2 + (m_0 c^2)^2$$

where E^2 and P^2 are the squares of the total energy and three momenta respectively. For a reaction with three free particles in the final state (1+2→3+4+5), with the masses known, the kinematical variables will have nine degrees of freedom. The four relations due to conservation of energy and momentum between the initial (1+2) and the final (3+4+5) states will reduce the number of independent kinematical variables to five. Due to azimuthal

independence the angle ϕ_3 can be set equal to zero degrees. Then a measurement of the kinetic energies T_3 and T_4, the polar angles θ_3 and θ_4 and the azimuthal angular difference θ_3-θ_4 will overdetermine the kinematics by one variable. Such an overdetermination serves to reduce the background and to remove a two-fold ambiguity. This ambiguity arises because the momentum of any nucleon in the final state can be expressed as a quadratic relation in the momentum of any one of the other final state nucleons.

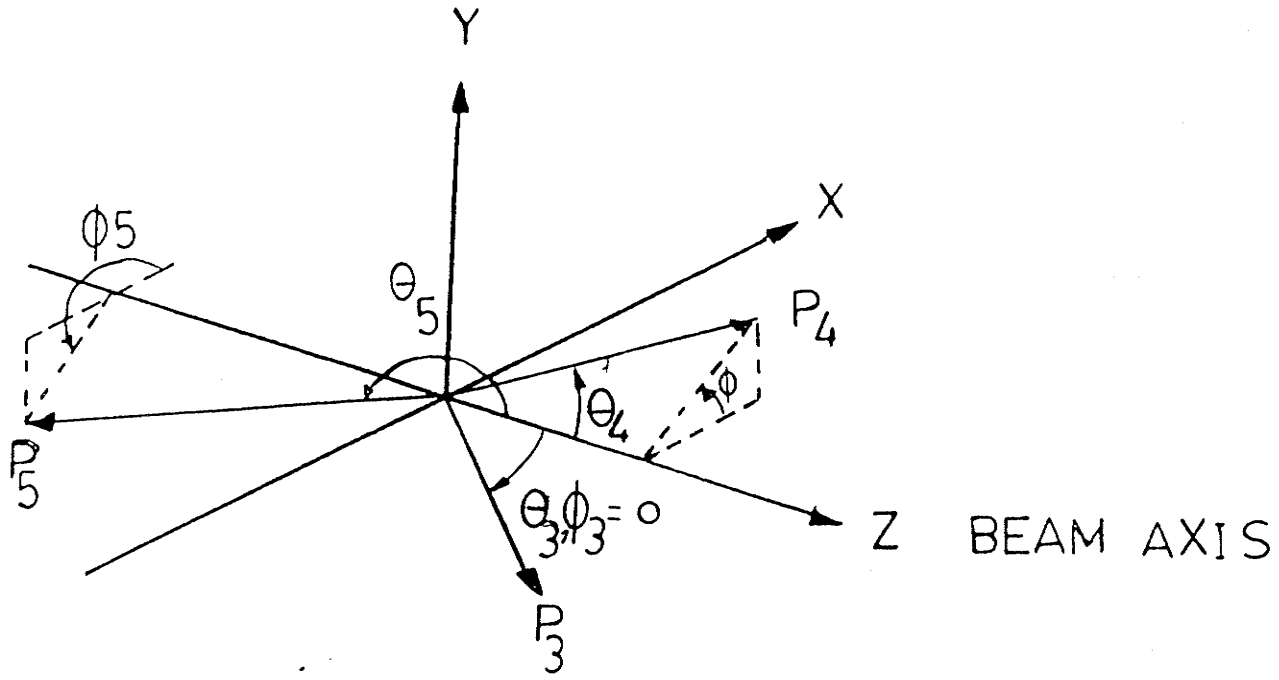

fig (2.1)

Definition of: the angles for a three-body reaction

P_3 in-plane, P_4 out-of-plane

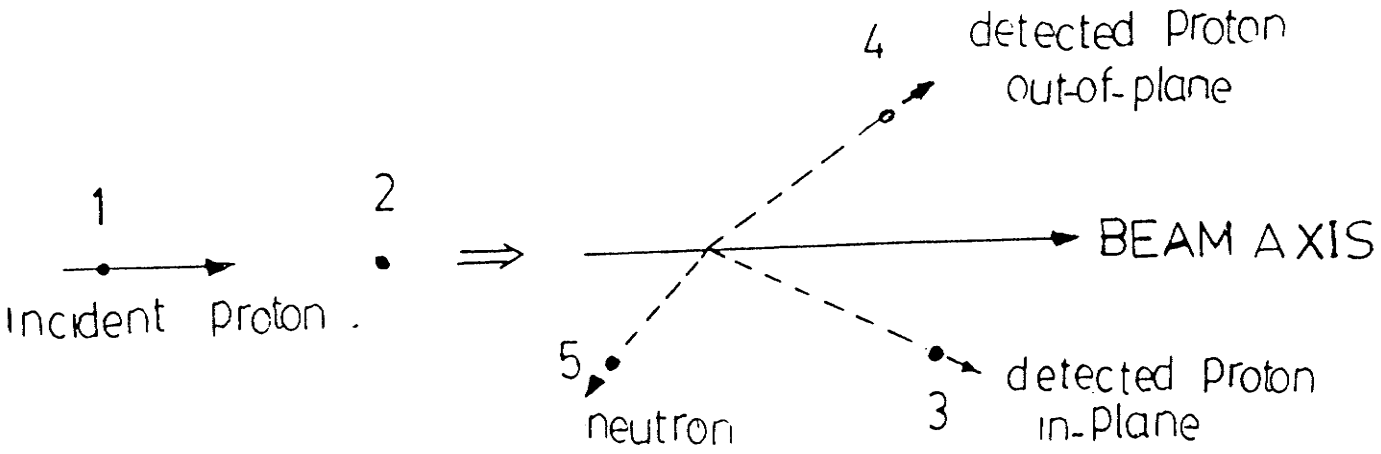

2 : deuterated PolyethYlene target

fig (2.2) Geometry of p+D ---> p+p+n

2.2 THE TREIMAN-YANG CRITERION AND ITS RELEVANCE TO THE DEUTERON BREAKUP REACTION

In general, the calculation of the total amplitude for a reaction of the type

$$A + X \longrightarrow B + Y + Z \qquad (2.2.1)$$

requires consideration of many competing processes, most of which depend upon five independent kinematic variables. If, however, it can be shown experimentally that the reaction is dominated by one particular exchange process then the calculation can be greatly simplified.

For example, the experimental conditions may be chosen so as to strongly favour the mechanism represented in the pole diagram of figure (2.2.1). It has been shown([1],[2]) that, provided the spin of the intermediate particle is 0, or ½ (in the non-relativistic case), the amplitude represented by fig (2.2.1) may be divided into two separate components corresponding to the two vertices of the graph. These are

$$A \longrightarrow B + i \qquad (2.2.2)$$

$$i + x \longrightarrow Y + Z \qquad (2.2.3)$$

The amplitude of eq. (2.2.1) now depends only upon three independent kinematic variables, all of which may be obtained from the vertex (2.2.3). These three quantities do not change if in the anti-laboratory system (i.e., that for which $P_x=o$), the momenta of particles Z and Y are rotated about the direction of the sum of their momenta. Thus, the only variation

in the differential cross section observed under such a rotation is due to the role of a phase space factor.

An experiment designed to study this effect constitutes a Treiman-Yang (TY) test. Originally, the test was thought to be valid only when the intermediate particle had zero spin. However, Shapiro([1]) has shown that it may also be applied to exchange processes involving particles of spin ½, provided relativistic effects are negligible.

Generally in three-body experiments one can enhance the process of interest geometrically by selecting a suitable region of cross section([5]). The question remains as to what extent observed spectra are due to contributions from a particular reaction mechanism and one pole graph is sufficient to describe them.

An experimental way of testing the basic assumptions underlying the spectator model was first demonstrated by Treiman and Yang([3]) originally for high-energy single pion exchange reactions, and extended later by Shapiro, Kolybasov and August([1,2]) for some non-relativistic cases involving particles of non-zero spin. This Treiman-Yang test has two characteristics: firstly the reaction amplitude is factorized, i.e., it can be written as the product of two amplitudes and a propagator, and secondly it depends on three variables instead of five. In the general case the first of these characteristics makes it possible to express the differential cross section of the reaction through that of the virtual process in the right hand vertex and the second enables us to indicate a simple method for identifying the pole mechanism experimentally([3]).

In order to use the Treiman-Yang criterion it is necessary to measure the direction of emission of the final particles and the energy of one of them. The connection between the differential cross section in the lab system and the square of the absolute value of the amplitude of the reaction can be readily obtained. This Treiman-Yang criterion, formulated to identify the nucleon exchange and depicted in figure (2.2.2), is performed most conveniently in the anti-lab system for the spectator being in the beam particle. Because this Treiman-Yang invariance is a necessary criterion any deviation would be the proof of contributions from other graphs.

Several experimental tests of the Treiman-Yang criterion in low-energy nuclear reactions have been made with different results([9],[10],[11],[12]). In Grenable a test has been made to identify the nucleon exchange pole and the test is made in the rest frame of proton P. 20 MeV deuterons are incident on a proton target and the two protons are detected in coincidence.

Our test has been made in the rest frame of the deuteron. A proton beam of 11.2 MeV was incident on a CD_2 target.

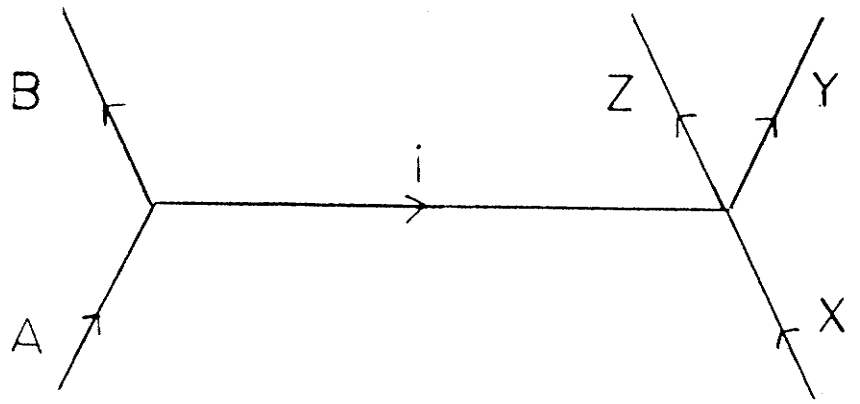

fig (2.2.1) An exchange pole diagram

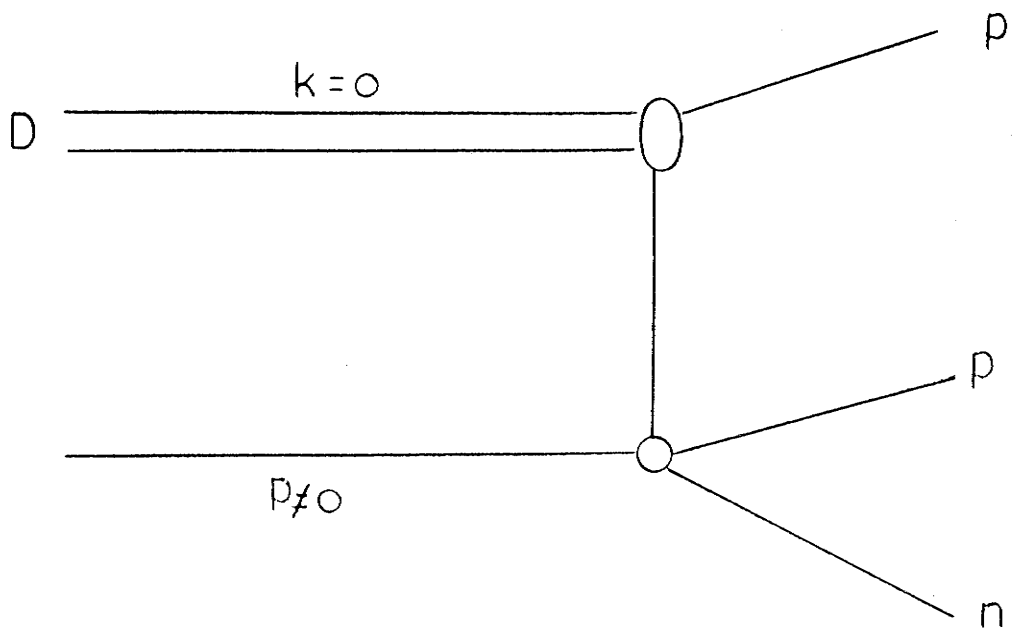

fig (2.2.2) Nucleon exchange pole diagram

2.3 THREE-BODY BREAKUP CALCULATIONS

The numerical solution of the Faddeev([49]) three body equations is greatly simplified if the two-body interaction is separable, in which case the Faddeev equations reduce to a set of coupled one-dimensional integral equations of the Lippmann-Schwinger type. Doleschall([27]) has succeeded in providing separable representations of the nucleon-nucleon interaction which not only give excellent fits to the nucleon-nucleon scattering phase shifts([15]) up to pion-production threshold, but also yield good results for nucleon-deuteron elastic scattering cross sections.

Computer programs developed by Doleschall([50]) have been used for the calculation of the nucleon-deuteron breakup cross section in the region studied in the present experiment. The nucleon-nucleon potential is taken as a sum of separable terms

$$\langle P(Ls)J\ (V)\ P'(L's')J\rangle=\sum_n g_n(Ls)J(P)\lambda_n g_n(L'S')J(P') \qquad (2.3.1)$$

Here L,S, and J are the two-body orbital, spin and total angular momenta. The two-body relative momentum P is defined in the way introduced by Lovelace([51]), so that P^2 is the two body relative energy. Thus, P has the units $(MeV)^{1/2}$. In the interaction of Doleschall([27,50]) used here the sum on n has at most 2 terms and the form factors g_n are taken([27]) to be

$$g_n(Ls)J(P)=K_{\eta L}P^l\ \frac{1+\sum_{i=1}^{N}\gamma_{nLi}p^{2i}}{\pi_{i=0}^{N}+L_{(1+\beta nLi)}P^2} \qquad (2.3.2)$$

For the energy used in this experiment, including s- and p- waves in the two-body interaction([26]) should be adequate. The $^3D_1$ partial wave is included because of its strong coupling to the $^3S_1$ wave via the tensor force which is important even at low energies, the parameters of this interaction being given in table (2.3.1).

Inclusion of the coulomb force([52]) in a three-body breakup calculation poses severe difficulties for the Faddeev theory. No correct treatment of this has as yet been found and known aproximation techniques are unreliable. For that reason, in the breakup calculations, the coulomb force is omitted since, as the coulomb force is long-range but relatively weak, it should have important effects only when the angle between the two outgoing charged particles is very small. For the kinematical conditions of this experiment, the coulomb force can be neglected.

Generally, the Doleschall code calculates all observables, but only the cross section used for this work and the results by Doleschall show a good agreement with three body data.

The form of the equation solved and the calculational techniques used by Doleschall([2]) can be summarized as follows:

The three distinguishable particles are considered as arbitrary masses m_i with spins σ_i. The two-particle interactions are labelled in the usual manner:

$$V_k = V_{ij} \qquad i,j = 1,2,3 \qquad k \neq i,j$$

the AGS([53]) form of the Faddeev equations is used

$$U_{ij}(w) = (1-S_{ij})(w-H_o) + \sum_{k=1}^{3} (1-S_{ik})\, T_k(w)\, G_o(w)\, U_{kj}(w) \quad (2.3.3)$$

$$\text{with } w = E + i\eta \ (\eta \to o), \quad G_o(w) = (w-H_o)^{-1}$$

$$T_k(w) = V_k + V_k G_o(w)\, T_k(w)$$

Here $U_{ij}(w)$ denotes the three-body transition operator, E denotes the energy of the three-particle system, H_o is the three particle kinetic-energy operator and $T_k(w)$ is the two-particle transition operator in the three-particle space. All these quantities and operators are understood to be in the three-particle c.m system. The indices i j of the transition operator $U_{ij}(w)$ denote the initial and final groupings of particles, namely in the ith grouping the ith particle is free and the other two are bound. In this notation the breakup channel is labelled with a zero index

$$U_{oj}(w) = w-H_o + \sum_{k=1}^{3} T_j(w) G_o(w) U_{kj}(w)$$

the coupled operator equations are treated in the momentum representation. The Lovelace([51]) momentum variables are introduced.

$$P_i = \epsilon_{ij} \frac{h(m_l k_j - m_j k_l)}{[2m_j m_l (m_j + m_l)]^{1/2}}$$

$$q_i = \frac{h\,[m_i(k_j + k_l) - (m_j + m_l)k_i]}{[2m_i M(m_j + m_l)]^{1/2}} \quad (2.3.4)$$

Where $i \neq j \neq l$, k_l is the wave number of ith particle.

$$M = m_1 + m_2 + m_3 \quad \text{and} \quad \varepsilon_{12} = \varepsilon_{23} = \varepsilon_{31} = 1,$$

$$\varepsilon_{ii} = 0, \quad \varepsilon_{21} = \varepsilon_{32} = \varepsilon_{13} = -1$$

There are three equivalent but none independent sets of variables P_i, q_i, that are connected via the relations

$$P_i = -A_{ij}P_j - E_{ij}B_{ij}q_j$$

$$q_i = E_{ij}B_{ij}P_j - A_{ij}Q_i \qquad (2.3.5)$$

where $A_{ij} = \left[\frac{m_i m_j}{(M-m_i)\ (M-m_j)}\right]^{1/2}$, $B_{ij} = \left[\frac{M(M-m_i-m_j)}{(M-m_i)\ (M-m_j)}\right]^{1/2}$

$$A_{ii} = -1 \ , \ B_{ii} = 0$$

The coefficients satisfy the identity ; $A^2_{ij} + B^2_{ij} = 1$. Including the spin variables denoted by $\vec{d} = d_1, d_2, d_3$ three two-particle $\langle P_i d_j d_k |$ bases $[i \neq j,k]$ and three equivalent three-particle $\langle p_i q_i d |$ bases are constructed after the usual angular-momentum decomposition, the $\langle Pi(L_i S_i)J_i |$ two-particle and $\langle P_i d_j (L_i S_i)\ J_i K_i L_i : J |$ three-particle bases are defined by the following relations

$$\langle P\ d\ d \mid = \sum_{L_i} \langle P\ (L\ S)J \ /\ \sum_{M_L M_S M_i} (E)^{S_l - \sigma_j - \sigma_k} \quad x$$
$$i\ j\ k \qquad\qquad i\ \ i\ i\ \ i \qquad\qquad jk$$

$$\langle \sigma_j d_j \sigma_k d_k | S_L M_s \rangle \langle L_i M_L S_i M_s | J_i M_i \rangle\ Y_{L_i M_L}(P_i)$$

$$\langle P\ q\ d \mid = \sum_{\substack{L_i S_i J_i \\ K_l l_i J^i}} \langle P\ Q\ (L\ S)J\ l\ :\ J / \sum_{\substack{M_i M_s M_i \\ M_k m_i M}} (E)^{S_i - \sigma_j - \sigma_k}$$
$$i\ i \qquad\qquad\qquad\qquad i\ i\ \ i\ i\ \ i\ i \qquad\qquad\qquad\qquad jk$$

$$\langle \sigma_j d_j \sigma_k d_k |\ S_i M_j \rangle \quad x$$

$$\langle L_i M_l S_i M_s |\ J_i M_i \rangle \langle J_i M_i \sigma_i d_i |\ K_i M_k \rangle \quad x$$

$$\langle K_i M_k L_i m_i |\ JM \rangle\ Y_{L_i M_i}(P_i)\ \ Y_{l_i m_i}(q_i)$$

Here $\langle L_1 M_1 L_2\ M_2 |\ JM \rangle$ is the Clebsch - Gordan coefficient. $Y_{lm}(p)$ are the spherical harmonics depending on the angles of vector P, the $L_i\ S_i J_i$ are relative orbital angular momentum, the total spin and the total angular momentum of the jk(i j,k) pair of particles respectively, the k_i are the channels spins, the l_i is the orbital angular momentum of the particle relative to the system of the jk pair and J denotes the total angular momentum of the three particle system.

Full details of the procedures to solve all the above equations and the calculational techniques are described by Doleschall[27].

Parameters in the separable interaction([27]) equations

partial wave	β_{nLi} (MeV^{-1})	γ_{nLi} (MeV^{-1})	K_{nL} ($MeV^{-1/2}$)	λ_n ($MeV^{-1/2}$)
$^1S_0$	1.7518×10^{-2}		1.0	-1.559×10^{-1}
$^3S_1$	2.089×10^{-2}	2.6670×10^{-2}	1.0	-1.6817×10^{-1}
$^3D_1$	2.500×10^{-2}	5.454×10^{-2}	-1.1987×10^{-2}	
	2.245×10^{-2}			
	1.221×10^{-2}			
	0.0			
$^3S_1$	2.438×10^{-2}	-8.7740×10^{-3}	-1.0	1.280×10^{-1}
	1.522×10^{-3}			
$^3D_1$	4.892×10^{-2}	2.499×10^{-2}	-2.8300×10^{-2}	
	1.146×10^{-2}			
	2.959×10^{-3}			
	1.631×10^{-3}			
$^1P_1$	2.2203×10^{-1}	5.4695×10^{-2}	1.0	1.6933×10^{-2}
	1.8889×10^{-3}			
	1.8860×10^{-3}			
$3P_0$	1.3317×10^{-1}	8.0240×10^{-2}	1.0	-5.4941×10^{-3}
	1.6727×10^{-2}			
	9.5283×10^{-3}			
$^3P_1$	1.0363×10^{-1}	2.4827×10^{-2}	1.0	1.9899×10^{-2}
	1.2209×10^{-3}			
	1.1877×10^{-3}			
$^3P_2$	9.1349×10^{-3}	3.2659×10^{-3}	1.0	-5.3872×10^{-4}
	1.8673×10^{-3}			
	1.4039×10^{-3}			

CHAPTER THREE

3.1 REVIEW OF PREVIOUS WORK ON DEUTERON BREAKUP BY PROTONS AND ITS INTERPRETATION.

A 10.0 MeV proton beam from the tandem accelerator in Uppsala has been used to study the proton correlation distributions from the d(p,pp)n reaction([16]). The electronic system allowed detection of protons down to 0.4 MeV. The angular resolution for each proton was 1.8° FWHM taking into account beam spot diameter and detector aperture.

Their results have been obtained for the following angular settings a) symmetric-coplanar, i.e., detectors in the same plane as the incident beam and at equal opposite angles $\theta_3=\theta_4=20°,25°,30°,35°,40°$ b) asymmetric-coplanar $\theta_3=30°,\theta_4=20°,25°,35°,40°,45°,50°,55°$ c) symmetric non-coplanar $\theta_3=\theta_4=30°$, $\phi_4=180°$, $\phi_2=0°$ to 90° in steps of 10° d) settings chosen to follow conditions for a Treiman-Yang test with $\theta_3=\theta_4=30°$. This means that most of the data have been obtained for kinematic conditions which traditionally have been considered to favour a quasi-free reaction mechanism.

A test has been made by Valkovic et al.([17]) to look for evidence for the quasi free mechanism in the low energy range from 7.0 to 13.0 MeV in the coplanar d(p,2p)n reaction with $\theta_3=\theta_4=30°$.

Recent successes have been seen in the analysis of the d(p,2p)n reaction with an exact solution of the three-body Faddeev equations. The

experimental results([16]) have been discussed with respect to the modified simple impulse approximation model([18]) in which the process is considered to be a quasi-free p-p scattering. The free p-p cross section has been chosen at the energy of the initial state of the proton pair and at the proper centre of mass angle for each point in the spectra.

The successful calculations by Ebonhoh([19]) on the d(p,2p)n reaction at 13.5 and 26 MeV, in which he solved the Faddeev equations exactly with a separable two-body interaction, makes it likely that coplanar results([16]) could also be explained in this way.

Deuteron breakup by the (p,2p) process was studied at Orsay([20]) at an energy of 156 MeV in a kinematically complete experiment over a wide range of neutron recoil momenta extending from zero (quasi-free scattering) to those for which off-energy shell effects and final state interactions are important([21]). The results were compared with calculations in the frame of the impulse approximation introducing the final state interactions for each pair of nucleons, and also the deuteron D state. This comparison could not explain the experimental cross sections in any kinematical condition, even for quasi-free scattering and concluded that multiple scattering in the final state interaction and off-energy shell effects must be taken into account([22]).

To substantiate these conclusions, and to obtain more information about the mechanism of the reaction, J.P. Didelez et al([20]) have undertaken a kinematically complete experiment in which the D(p,2p)n and D(p,pn)p reactions are compared under the same experimental conditions. The experiment was carried out using the 156 MeV extracted proton beam of the Orsay synchro-cyclotron. They used a cylindrical liquid deuterium target of 18 mm diameter and 60 mm height contained in a 8 mm Havar cell. The two scattered protons (for the p,2p reaction) or a proton and a neutron (for the p,pn reaction) were detected in coincidence at angles θ_1 and θ_2.

They observed that in the QFS region, it was confirmed that the spectator model could not explain the experimental cross sections in all the kinematical conditions.

An extensive series of deuteron breakup experiments has also been performed at the Naval Research Laboratory sector focusing cyclotron([23]) at an energy at 23 MeV. Their work was initiated after an experimental study of the reaction D(p,pn)p at UCLA showed that some of the features of the reaction could not be understood even in a qualitative manner([24]). The initial NRL study investigated the energy dependence of the p-n quasi-elastic scattering process([25]). At the same time other laboratories were doing similar studies for the p-p QES([18]). The cross sections for the two processes differ both in magnitude and in the energy dependence and are not compatible with the simple impulse approximation. Up until now there have been a number of theoretical and experimental investigations for QE deuteron breakup. All of these have been able to show calculated spectra that, usually renormalized, nearly fit experimental results. A deuteron

breakup theory to be viable, must fit the cross section magnitude, the angular distribution and the spectral shapes for both pp and pn data.

In Birmingham([13]) the H(d,pn)p reaction has been studied in the vicinity of the kinematic region for quasi-free p-p scattering. A Treiman-Yang test carried out at an incident deuteron energy of 12.2 MeV and for low momentum transfer to the proton target, shows that nucleon exchange is the dominant process under their conditions.

This experiment was designed to study the Treiman-Yang criterion for nucleon transfer, the experiment was designed so that i) their measurements were close to the p-p quasi-free scattering region. Ideally the spectator neutron should emerge with about half the incident deuteron energy ii) the momentum transfer q from the deuteron to the proton was as low as possible $q = Pn - \frac{1}{2}P_o$ where P_o is the incident deuteron momentum and P_n the momentum of spectator neutron iii) the possibility of final state interactions was minimized by achieving large relative momenta between pairs of particles. They concluded that, under the conditions of low momentum transfer and quasi-free p-p scattering, the nucleon exchange pole favoured under experimental conditions satisfactorily describes the mechanism of the reaction d + p → p+p+n.

Exact calculations are possible in the three-nucleon system. The Faddeev three-body equations have been solved by several groups both for nucleon-deuteron elastic scattering and for nucleon-deuteron break up while many early exact three-body calculations used s-wave nucleon interactions([28],[29]), others have included higher partial waves.([27],[30],[31]) Good agreement with cross section and polarization data at 10, 14.1 and 22.7 MeV has been obtained using local and non-local separable interactions([32]) including s,p and d partial waves. With similar interactions satisfactory results have been obtained([31]) for nucleon-deuteron break up cross sections at 22.7 MeV in the vicinity of the quasi-free and final state interaction peaks.

The $^{2}H(p,2p)n$ reaction (Birchall et al.) was studied using the University of Manitoba Spiral Ridge Cyclotron Facility as a kinematically complete experiment at an incident proton energy of 28.6 MeV to investigate spectra of p-d breakup in collinear geometry. The two outgoing protons were detected in coincidence in ΔE-E telescopes on either side of the beam at three different pairs of angles. Two of the angle pairs (58.5° - 58.5° and 54.6° - 62.5°) correspond to collinear geometry at one point on the break up kinematic locus and the third angle pair (54.6°-54.6°) has no collinear point. The results were compared with an exact three body calculation using the Doleschall code([27]). The calculation includes two-body interactions in s and p waves, agreement with the experiment is excellent.

CHAPTER FOUR

THE EXPERIMENT

4.1A PREPARATION OF DEUTERATED-POLYETHYLENE TARGETS

A method is now preferred for the preparation of deuterated polyethylene targets in the 1-5 mg/cm^2 thickness range([45]). The targets obtained are uniform, the following is the recipe used:

First 100 mg of CD_2 is dissolved in 20 ml of xylene. This is accomplished slowly in a covered beaker on a hot plate at 140-150° C. Once dissolved, a "stiff" solution is obtained which when allowed to cool slightly, forming a gel. The near boiling solution is poured onto a glass slide (7.5 x 3.8 cm^2 typically used), which has been precoated with a soap solution, in just sufficient quantity to cover the slide. The slide is not heated but every few minutes the slide is covered with a further layer of hot solution until the desired thickness is reached. Once formed the film is floated off the slide using a water bath.

The advantage of the method is that a well polymerized foil can be obtained without heating the foil. It appears that maintaining the deuterated polyethylene in a plastic state during evaporation of the xylene promotes polymerization. This can be achieved by heating the glass slide on which the foil is made but has often one disadvantage particularly with thicker foils, that the solution can boil on the slide causing non-uniformity in the foil thickness.

4.1B THE MANITOBA CYCLOTRON FACILITY

The University of Manitoba spiral ridge cyclotron([33],[34],[35],[36]) is a sector focused machine with accelerating electrodes (dees) confined to the valleys. The acceleration of negative hydrogen ions([37]) allows one to obtain external proton beams variable in energy from 22 MeV to 50 MeV. The variable energy extraction probe is similar to the system([38]) developed for the UCLA cyclotron. The stripping foil (0.0005 inch thick aluminum) removes both electrons from circulating H^- ions with a consequent reversal of the radius of curvature of the resultant protons in the magnetic field of the cyclotron. The use of negative ion stripping preserves beam quality, has a high extraction efficiency, ~ 100 %, and allows rapid energy variation without changing the magnetic field and radio-frequency acceleration of the cyclotron. The radial motion of the stripping foil provides the energy variation while the azimuthal motion of the foil ensures that the various proton trajectories intersect at a common point outside the magnetic field of the cyclotron. At this location a bending magnet (CM) directs the protons along the external beam transport system, see figure (4.1.1).

The present experiment was performed using the 28 inch scattering chamber located on the 45° right beam line from the switching magnet (SW). A horizontal waist is produced in the proton beam at the aperture of the slit system, (S1) by the quadrupole doublet (Q_1, Q_2). The slit system (S1) is located in the object plane of the bending magnet (SW). The beam entering the bending magnet has a typical energy spread of 0.5 to 1.0 MeV([39]). The energy analysis slits (S2) are located at the focal plane of the bending magnet. Another quadrupole doublet (Q_9,Q_{10}) then produces a

double waist in the beam at the center of the scattering chamber. The size and momentum spread of the beam spot depend on the apertures of slits (S1) and (S2). The object slit (S1) was set at 0.2 inches wide by 0.8 inches high while the image slit (S2) was 0.1 inches wide by 0.2 inches high. The beam spot size was approximately 2 mm wide by 4 mm high. Due to stray residual magnetic fields induced in the steel shielding between the 28 inch chamber and the high resolution beam line it was necessary to employ a horizontal steering magnet at the exit of the last quadrupole doublet.

The cross-over method([40],[41]) was used to relate the magnetic field of the bending magnet to the energy of the analysed beam([42]). For the cross-over method a 2.54 mg/cm^2 thick CH_2 target was used. The beam energy was determined by selecting nominal incident energies in the range 20 to 40 MeV and then measuring the cross-over angle for protons scattered from hydrogen and the first excited state of Carbon-12 (4.43 MeV). The field strength of the bending magnet is determined by an NMR probe located between the magnet poles. The NMR frequency ν is linearly related to the proton momentum p in the magnet, i.e., ν_{NMR} = constant *p. The accuracy of momentum calibration was $\frac{\delta P}{p} = \pm 0.15$ %.

As a further check on the calibration([42]) the incident beam energy was increased by small energy increments through the well known $J^{\pi} = \frac{3}{2}^+$ resonance in ^{5}Li. This state is excited at an incident proton energy of 23.45 MeV. This gave agreement with the NMR calibration to within 25 keV([41]).

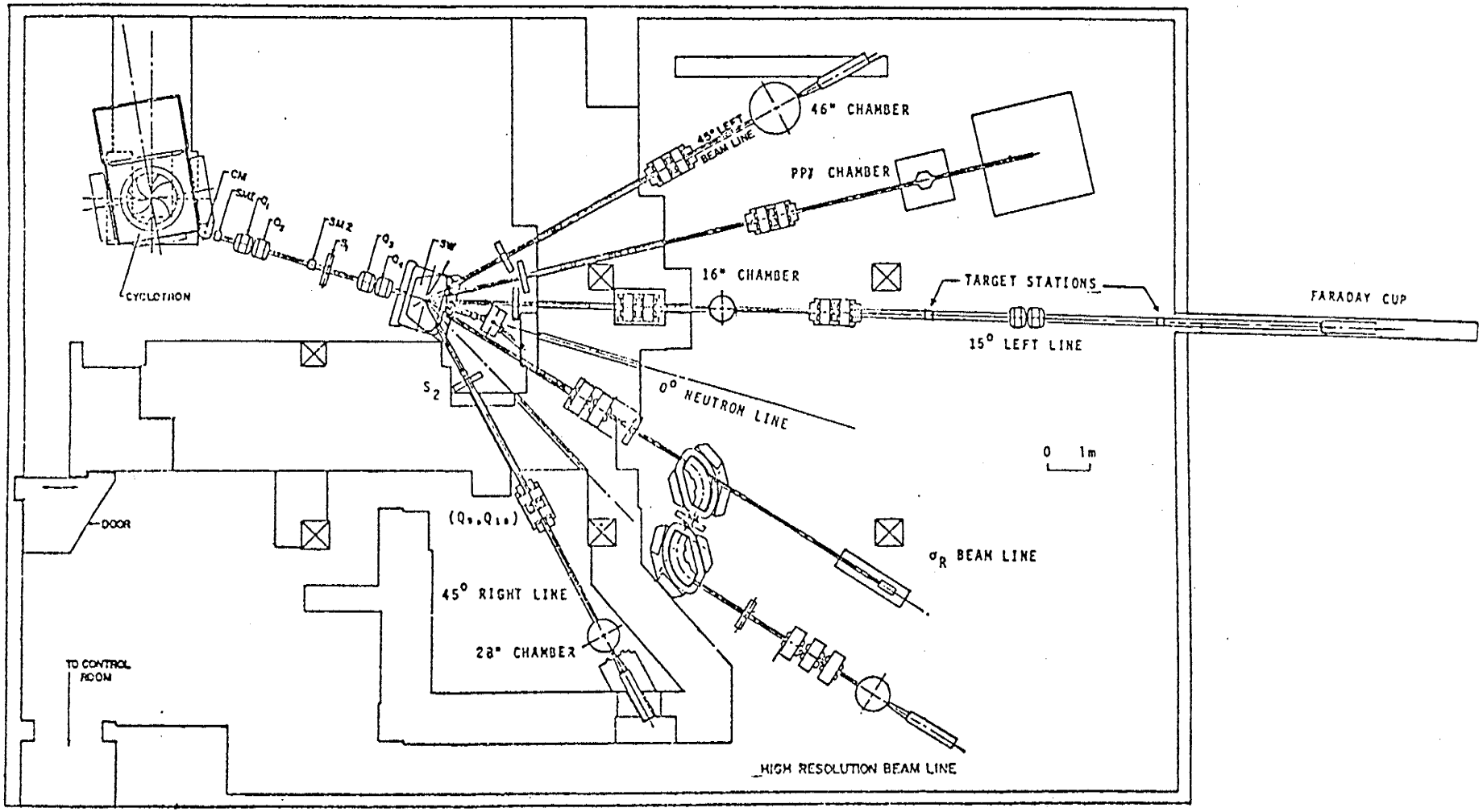

Scale drawing of the cyclotron layout (1974). The Non-Coplanar equipment was located in the 45° right line area.

fig. (4.1.1)

4.2 THE 45 DEGREE RIGHT BEAM LINE AREA

A global view of the 28 inch scattering chamber and support equipment is presented in the photograph figure (4.2.1). The 14 inch diameter cylindrical shell on top of the chamber houses the non-coplanar apparatus. The other photograph figure (4.2.2) shows the inside of the 28 inch chamber. It contains two horizontal turntables which can be rotated independently between -180° and +180°. Remote readout for the angle of rotation of the turntables is supplied by two Decitrak shaft encoders which have an angular precision of ±0.05°. Each turntable supports a brass detector holder. Counter telescopes are accurately positioned on these platforms by dowel pins. A deuterated-polyethylene target placed on the plate of the cell which attaches to the non-coplanar equipment has been placed at the centre of the chamber in the photograph to illustrate its relationship to the in-plane counter telescope([42]). Details of the non-coplanar counter telescope are visible in figure (4.2.2). The out-of-plane collimator is maintained perpendicular to the scattering plane for the detected particle by the small motor next to the snout. In order to reduce the problem of ground loop noise in the solid state detector circuits the detectors were electrically isolated from the chamber.

The proton beam leaves the chamber via a 50 μm thick kapton H foil exit port, passes through a 4.0 cm air gap and enters a 1.8 metre long Faraday cup which also has a 50 μm thick kapton H foil entrance window. The impedance between the steel casing of the Faraday cup and its central carbon core is 10^{15} ohms. Inside the Faraday cup, a copper suppressor ring was maintained at -1.5 kV with respect to the steel casing. This prevents

secondary electrons from entering or leaving the carbon core. The beam current was monitored by a charge integrator (Brookhaven Instrument Corp. model 1000) with a quoted accuracy of 0.2 %.

fig. (4.2.1) Non-coplanar apparatus

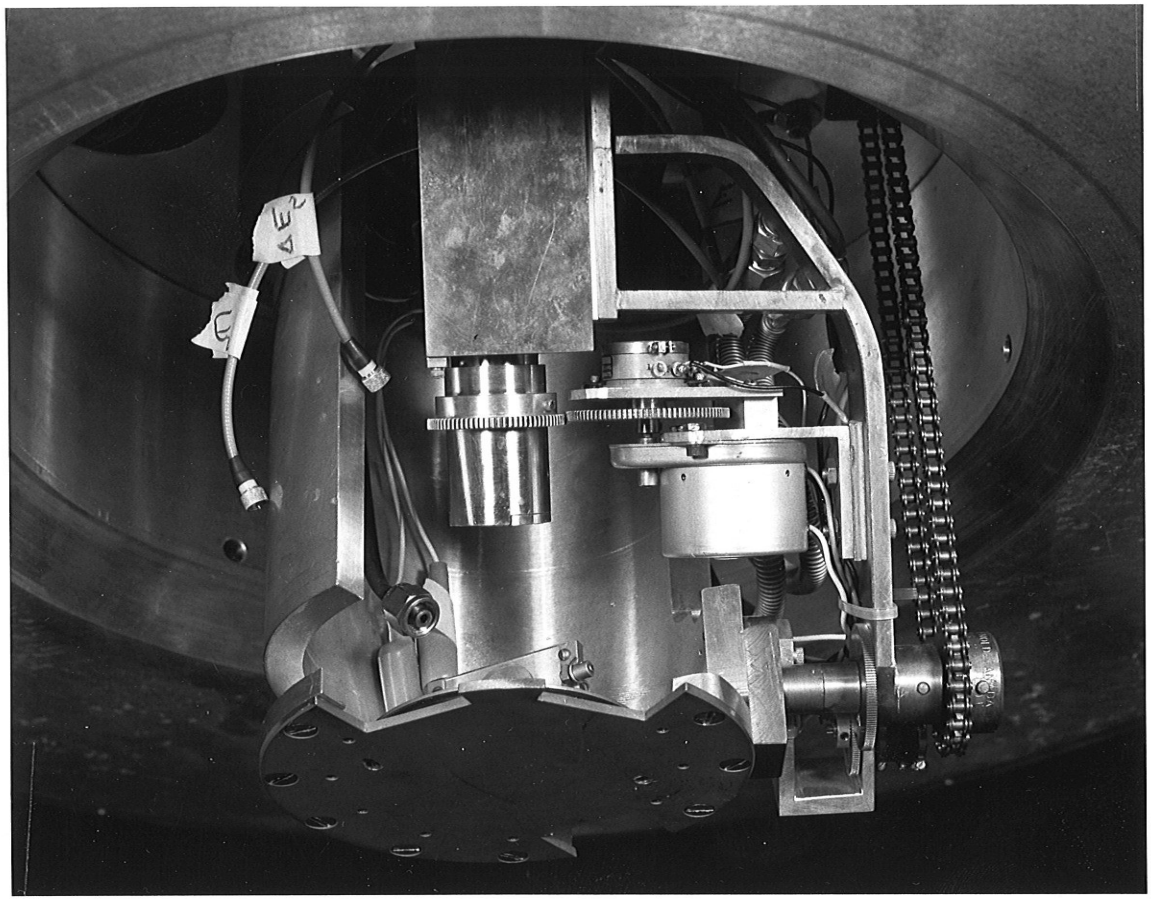

Central column of the out-of-plane assembly

fig. (4.4.2)

4.3 SET UP AND CALIBRATION

Prior to data collection, several setup procedures are necessary. Before the non-coplanar assembly is installed on the 28 inch chamber the beam optics are adjusted. The beam spot, typically 2 mm wide by 4 mm high, is viewed on a plastic scintillation screen (NE-102) located at the centre of the chamber.

After beam alignment, the non-coplanar detector assembly was lowered into position. This assembly had previously been aligned with the scattering chamber evacuated to ~ 10^{-2} torr. Alignment under vacuum was essential due to the compressive forces on the chamber. Prior to the start of the experiment the non-coplanar angular (α,β) readout had been set. See figure (4.3.1) for the definition of these angles.

The initial energy calibration of both counter telescopes was set up by an Ortec 448 precision pulser. The final energy calibration and determination of zero offsets were made by looking at p-p and p-d coincidence events.

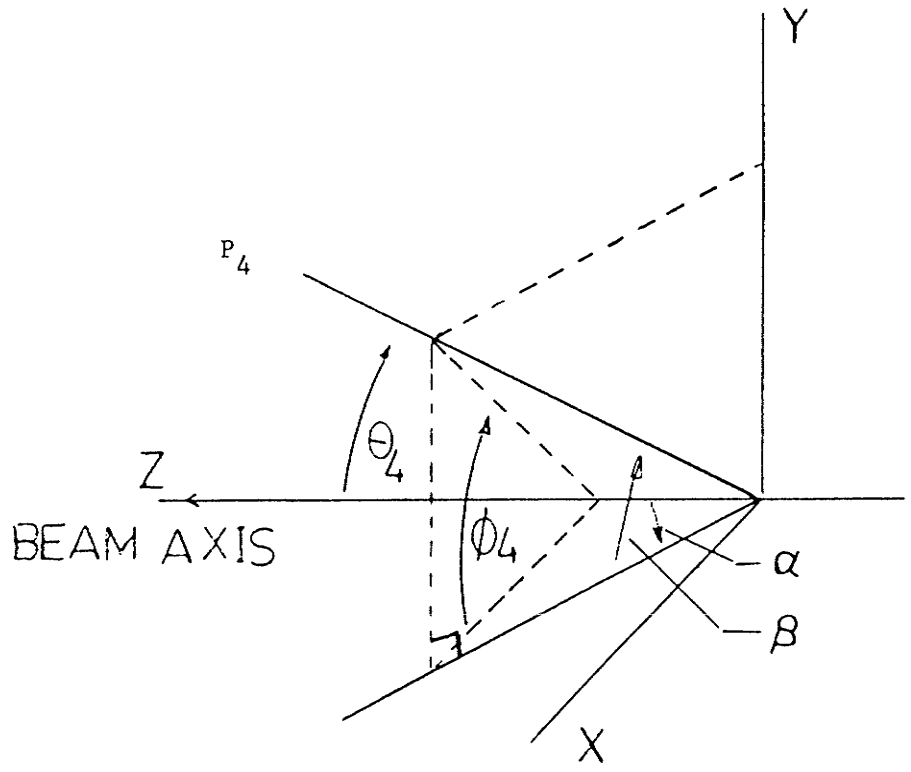

α = ARC TAN (TANΘ_4 * COSϕ_4)

β = ARC TAN (sinθ_4 * sinϕ_4)

fig (4.3.1) Relationship between the non-coplanar equipment angle setting (α_1,β_1) and the scattering angle (θ_4,ϕ_4)

4.4 DETECTOR ASSEMBLY

The two counter telescopes were of similar construction, see figure (4.4.1). To reduce pick up from ground loops the detectors were mounted in the brass cubes by perspex rings to provide electrical insulation.

Silicon surface barrier detectors 100 μm thick (from Ortec) were selected as ΔE counters. This thickness will stop 3.2 MeV protons and has an energy loss of about 1 MeV for 9 MeV protons. These detectors will provide a) a pulse large enough to exceed noise level for the proton energies of interest and yet b) not introduce too high a low energy cut-off and c) provide adequate separation between protons and deuterons of the same energy on a two-dimensional ΔE versus E + ΔE pulse height spectrum. An additional advantage of surface barrier detectors is their high resistance to neutron damage, an important factor in the present experiment.

The veto detector (2000 μm) rejected particles, mainly elastically scattered protons, which had sufficient energy to penetrate the combined thickness of the ΔE and E detectors. The E detectors used were 500 μm which, together with the ΔE detectors, stop 9 MeV protons.

A double set of collimating slits was used, a brass cylinder connects the front and rear collimating slits to exclude from the detectors some events which originate in the edges of the target holder. Nickel was selected for the collimators in the out-of-plane telescope since among common materials, including tantalum, it has the lowest slit edge-scattering for a given thickness([43],[44]). The dimensions of the collimator apertures used are given in table (4.4.1).

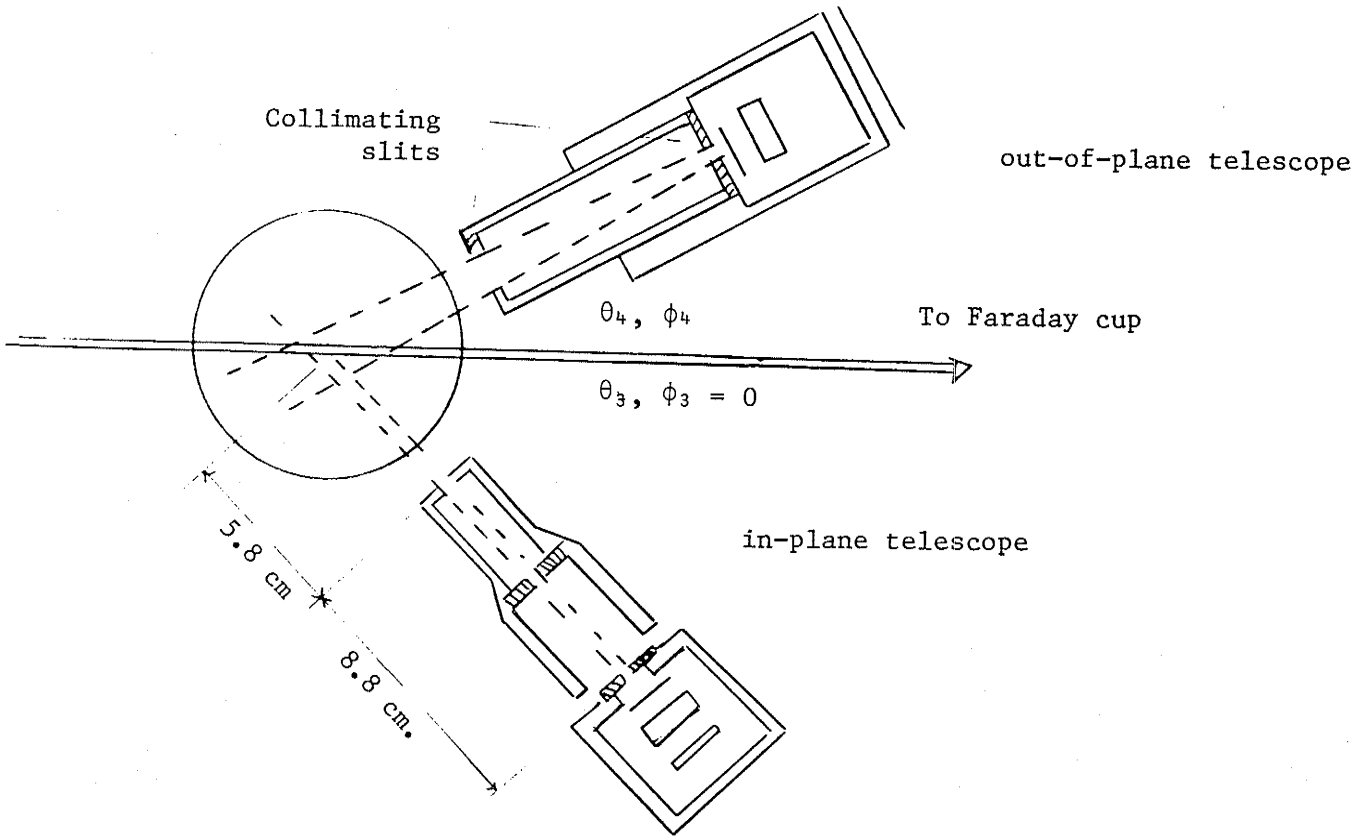

fig (4.4.1) Drawing of the detector telescopes and the slit system

Geometry of the in-plane and out-of-plane collimators

	In-plane	Out-of-plane
Front slit		
height (cm)	0.72	1.598 cm (diameter)
width (cm)	0.767	
Rear slit		
Diameter (cm)	0.584	width (cm) 0.402
		height (cm) 0.597
Solid angle		
($x10^{-3}$Sr)	0.286	1.106

Distance between slits = 8.8 cm

Distance of back slits from target centre = 14.6 cm

Table (4.4.1)

4.5 THE ELECTRONICS

A block diagram of the electronics is shown in figures (4.5.1, 4.5.2, 4.5.3). Commercial units in standard NIM bins were used. Initial pulse amplification was provided by five Ortec 100A charge sensitive pre-amplifiers located next to the scattering chamber. The signals were then transmitted to the control room where the main electronics and VAX 11-750 computer were located. All pulse height information signals were amplified by Ortec shaping amplifiers. To allow greater use of the dynamic range of these amplifiers and consequently to simplify particle identification by software, the ΔE pulse after division by 8 is added linearly to the E pulse to provide an ADC input signal.

The pre-amplifier outputs of the ΔE detectors (in-plane and out-of-plane) were fed to timing filter amplifiers (TFA) to generate a fast timing pulse. The TFA outputs entered the "start" and "stop" channels of a Time to Amplitude Converter (TAC), so that random and prompt plus random coincidence events between the in-plane and out-of-plane telescopes could be observed (ΔT signal).

The timing information contained in the ΔT signals was extracted using a combination of an Ortec 454 variable band-pass timing filter amplifier and an Ortec 453 constant fraction pulse height discriminator.

The two resulting timing-signals start and stop an Ortec Time to Amplitude Converter (TAC) set on the 100 nsec. range. The output of the SCA, the TAC output is the ΔT signal generated as a master coincidence pulse which opened the ADC linear gates to initiate event processing.

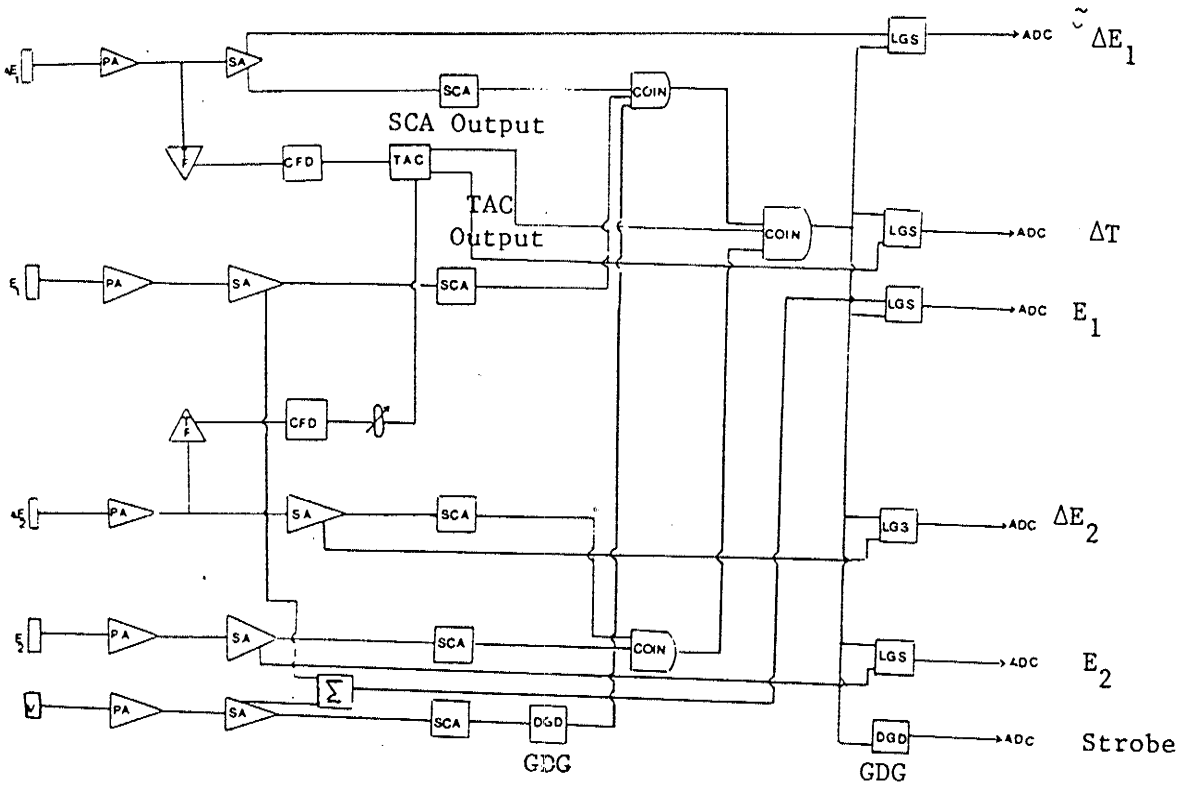

DA charge sensitive preamplifier
SA shaping amplifier
TF timing filter amplifier

coincidence

summing amplifier

fig.(4.5.1)Block diagram of the electronics system for the $^{2}H(p,2p)n$ experiment

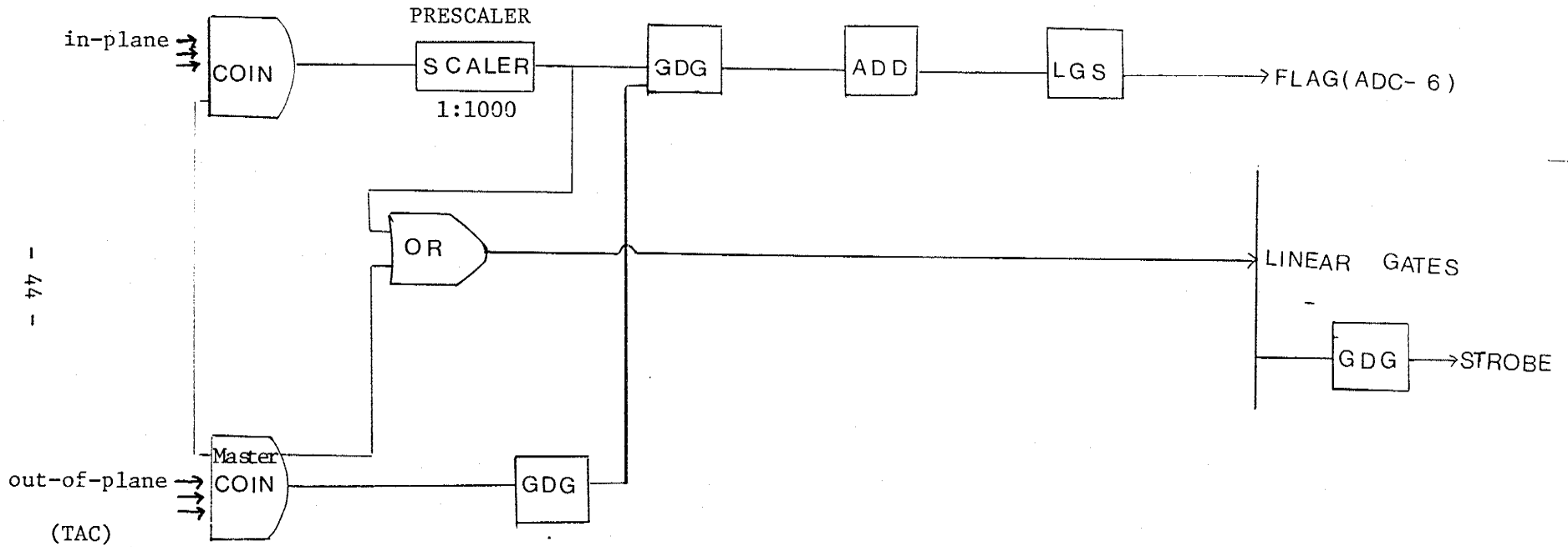

Sampling of fraction of elastic protons

fig. (4.5.2)

Identification of Monitor and Breakup Events

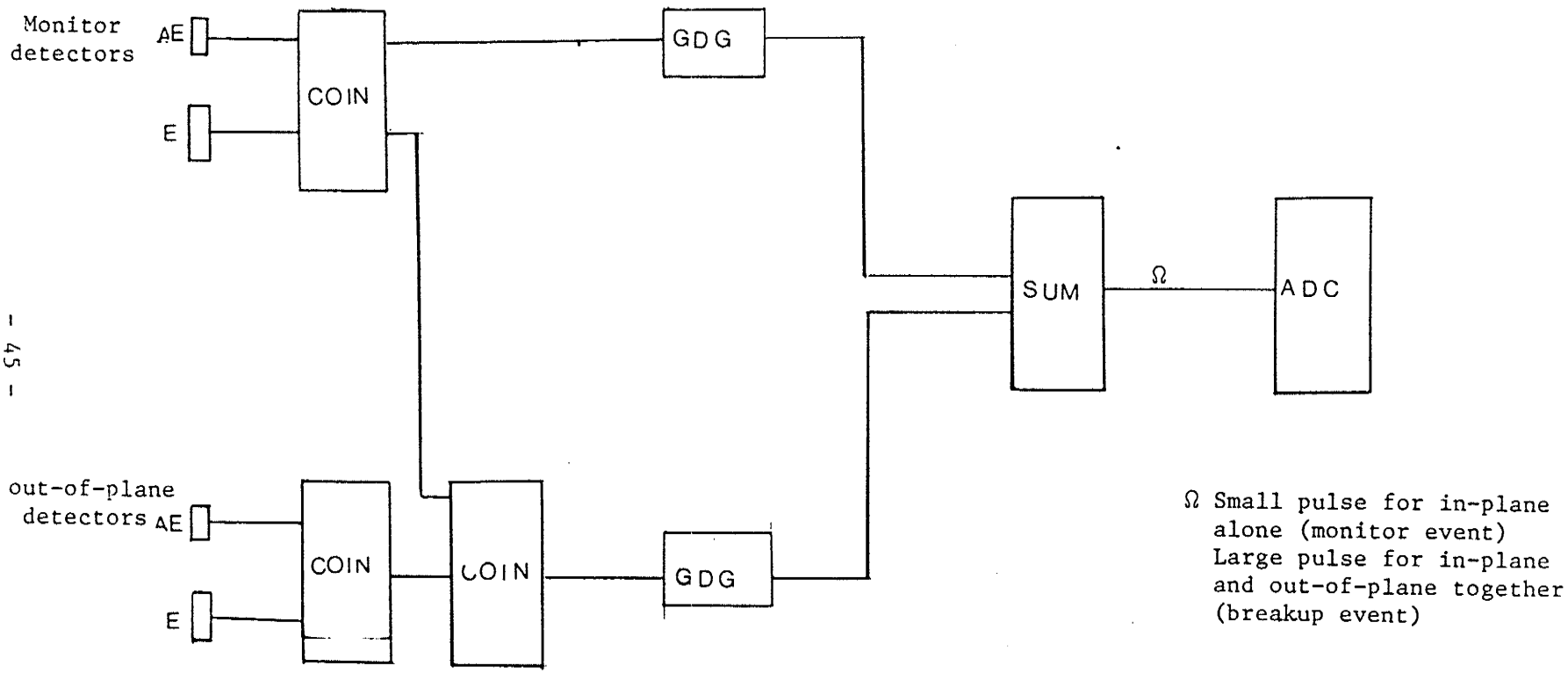

fig. (4.5.3)

4.6 SOFTWARE FOR DATA COLLECTION

A program was used for 1) multi-parameter data acquisition and 2) online analysis and display. The program was written specifically for the present experiment (by Jim Birchall) and will perform particle identification and store processed data words in various regions of the computer memory. All data are stored in unprocessed form on magnetic tape for further off-line analysis. This avoids the loss of information resulting from any error during online processing.

A number of displays of 64 x 64 arrays stored in the computer memory were available during data collection. The axes of these arrays correspond to the in-plane and out-of-plane energies and E-ΔE plots to identify proton events.

The signals were fed to the VAX via a multiparameter ADC for in-plane and for out-of-plane ΔE signals.

Plots of E versus ΔE for in-plane and out-of-plane telescopes were used to select proton events in the two telescopes. Events in the 15° fixed angle detector, for which there were in-plane signals but no corresponding out-of-plane signals were used to monitor the product of integrated beam current and target thickness. For events in which both in-plane and out-of-plane signals were present, spectra were set up for "true plus random" events and "random" events according to whether the event in the ΔT spectrum lay in the prompt coincidence peak or in one of the random coincidence peaks.

After selection of prompt proton events in the two telescopes and the construction of a 64 x 64 channel spectrum of E in-plane against E out-of-plane, a one dimensional spectrum was formed by projecting the two-dimensional spectrum onto the in-plane energy axis. (fig. 4.6.1-4.6.6)

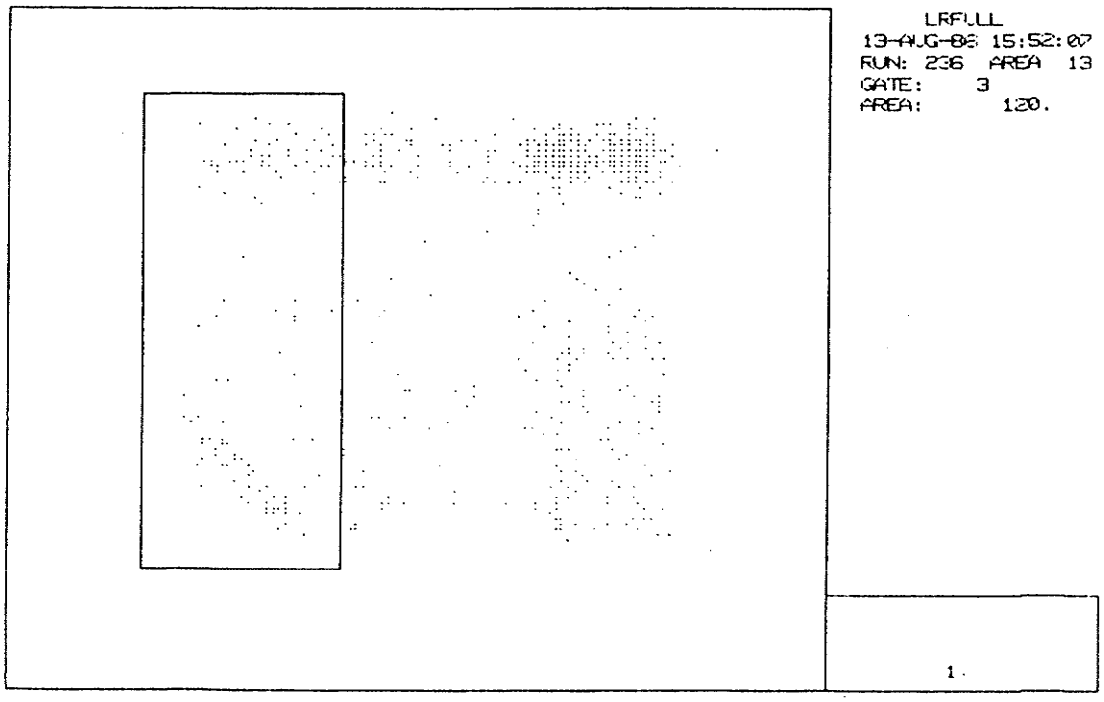

NOTE: Window used to avoid projecting random events into events of interest.

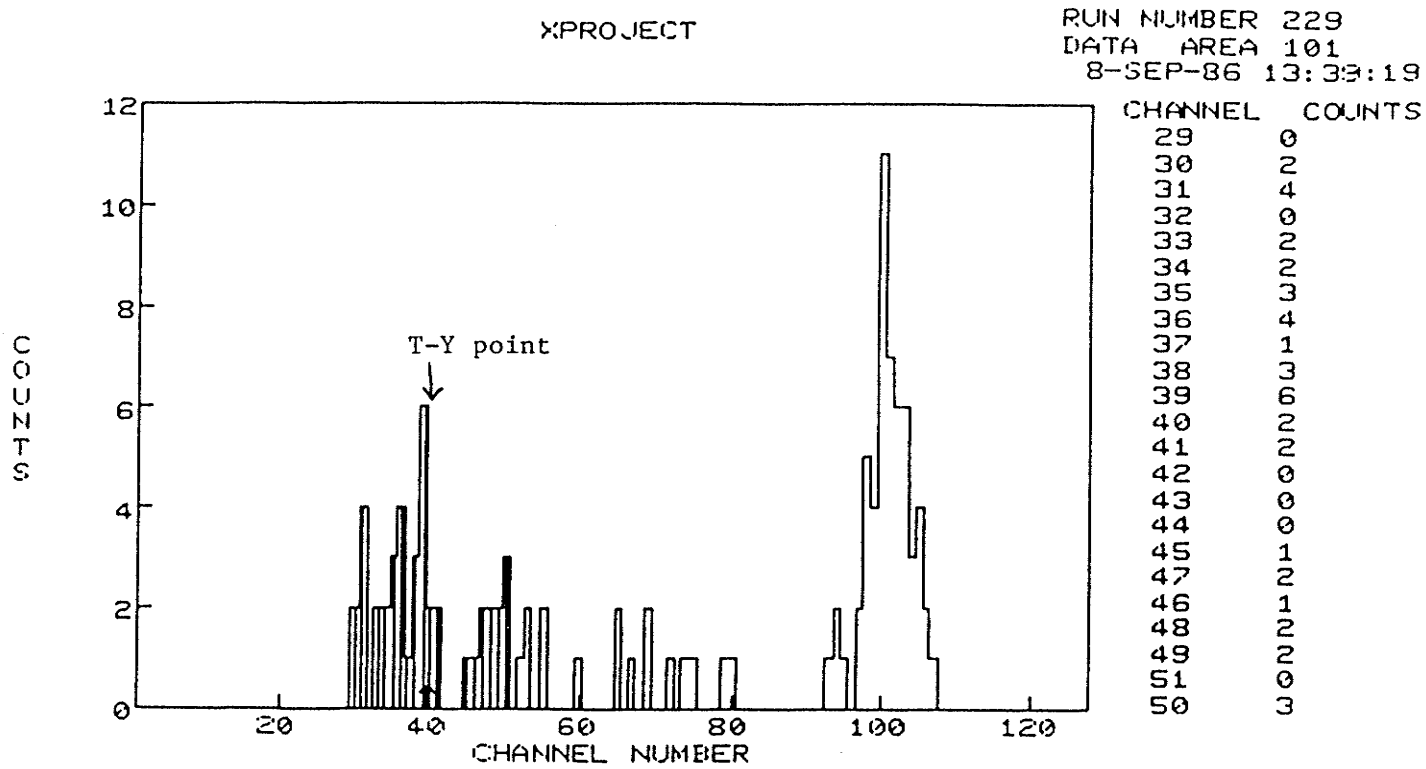

fig. (4.6.1) Projection onto E axis of proton-deuteron breakup spectra

(Treiman-Yang angle $\varepsilon = 30^{o}$)

The Treiman-Yang point is indicated by the arrow.

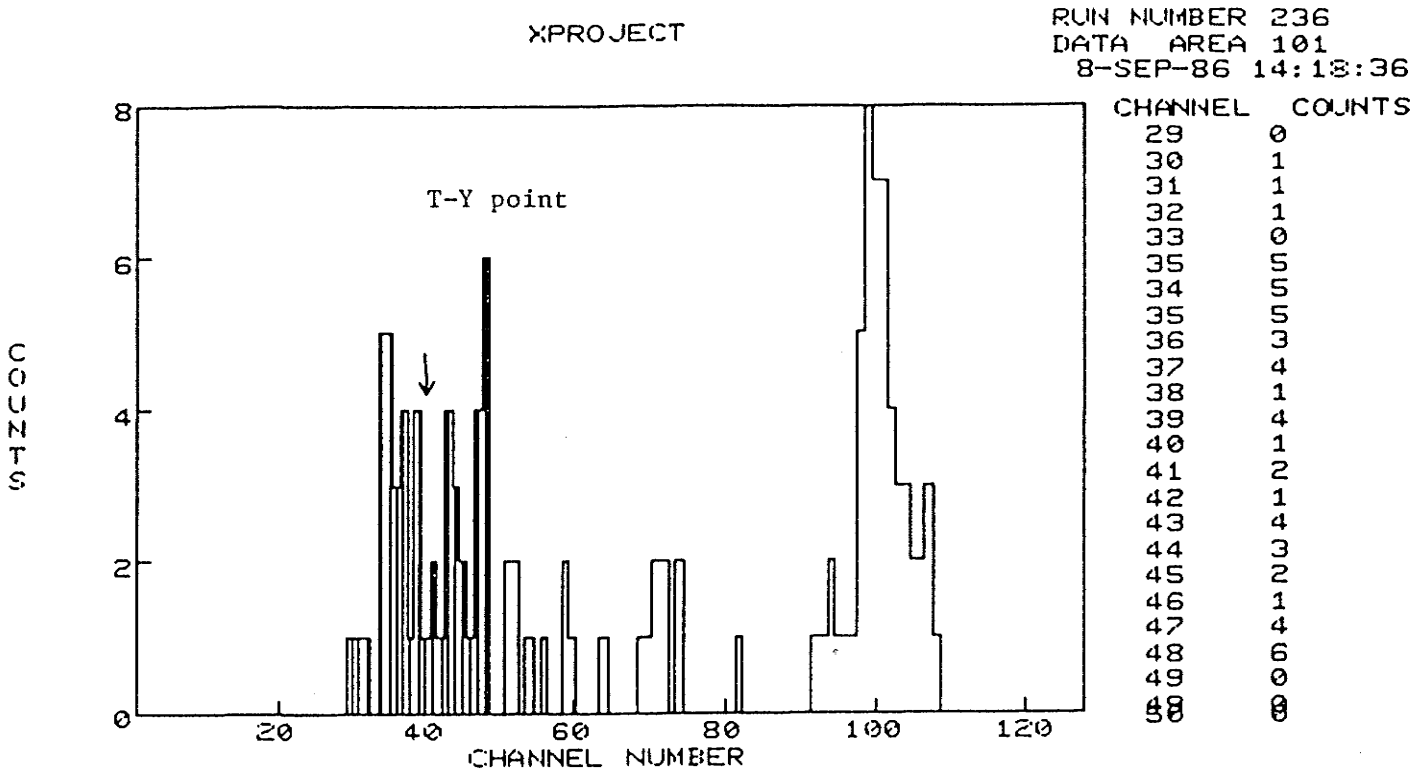

fig. (4.6.2) Projection onto E axis of proton-deuteron breakup

(Treiman-Yang angle $\varepsilon = 45^{o}$)

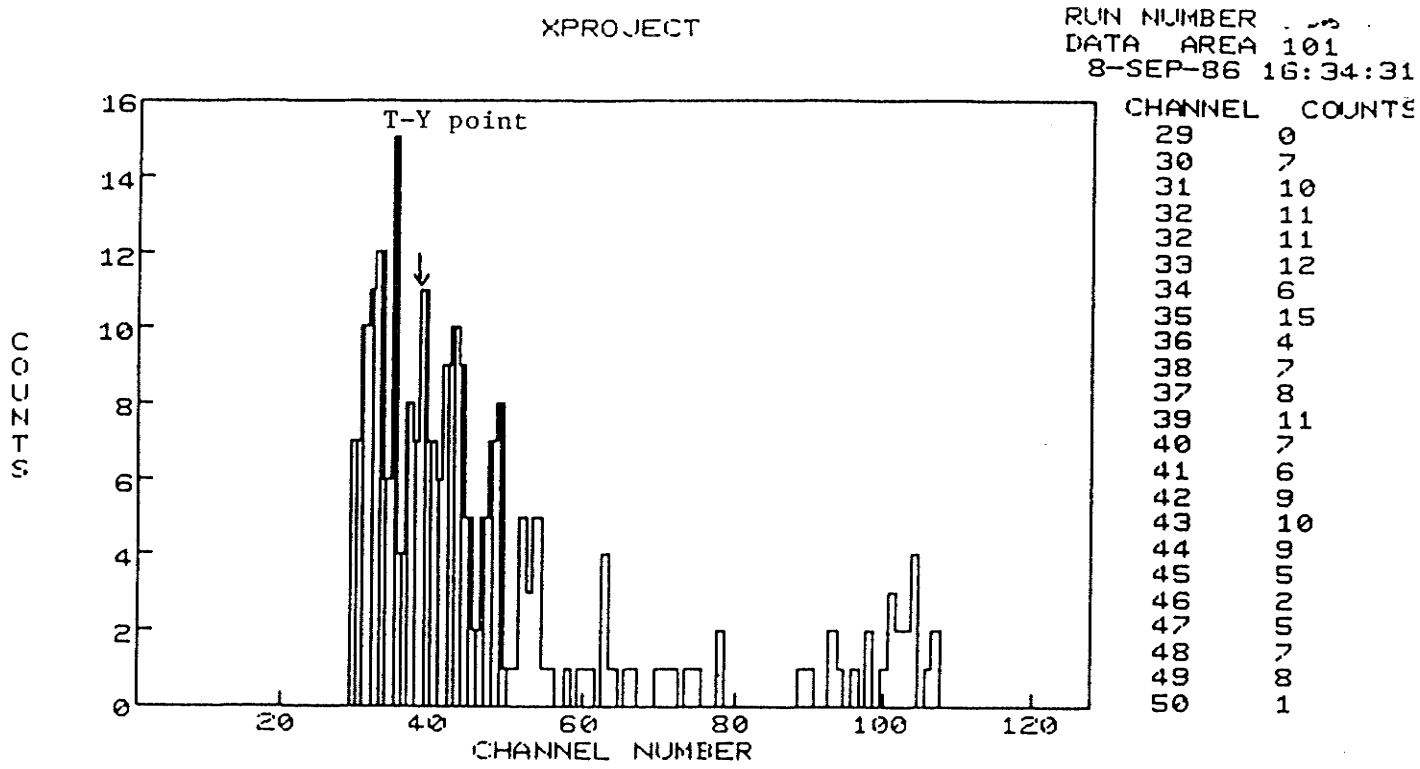

fig. (4.6.3) Projection onto E axis of proton-deuteron breakup spectra

(Treiman-Yang angle $\varepsilon = 60^{o}$)

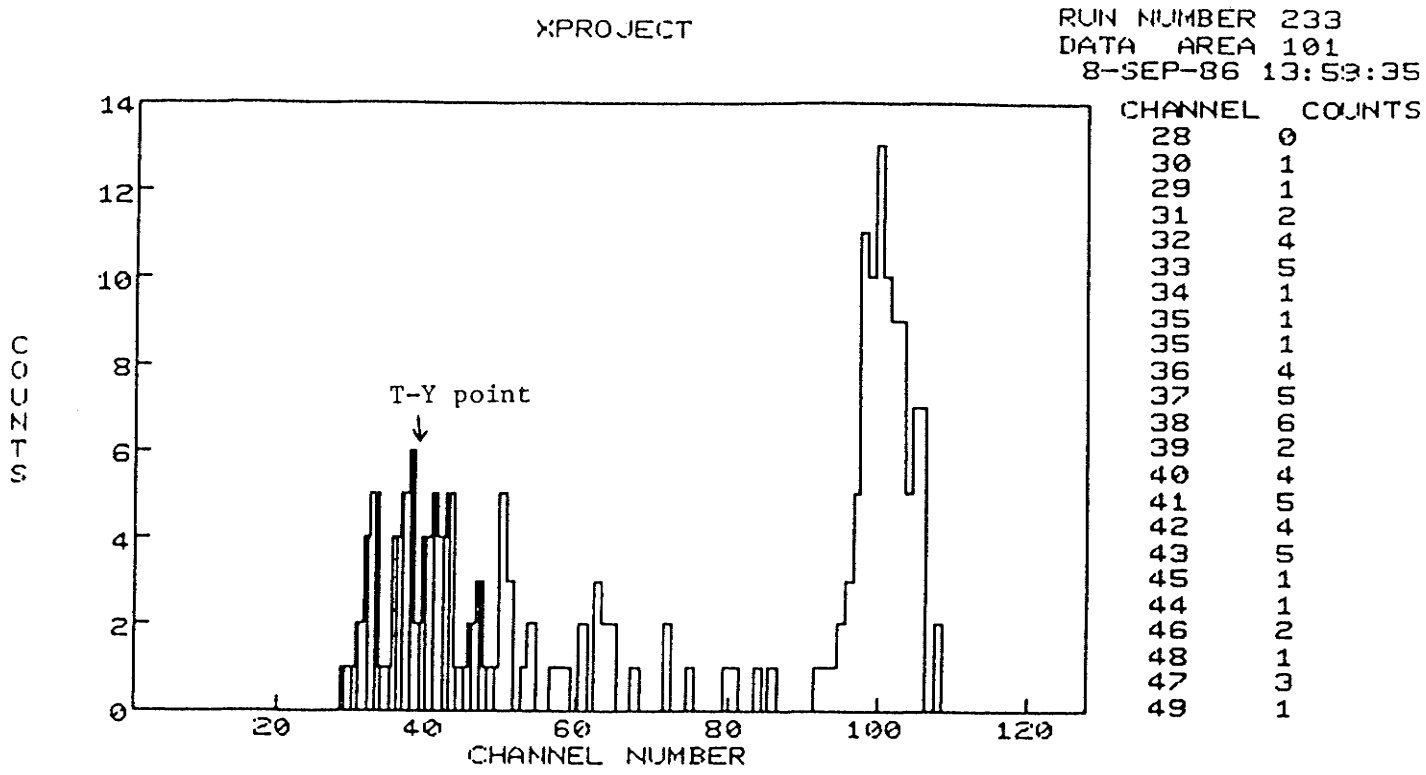

fig. (4.6.4) Projection onto E axis of proton-deuteron breakup spectra

(Treiman-Yang angle $\varepsilon = 75^{o}$)

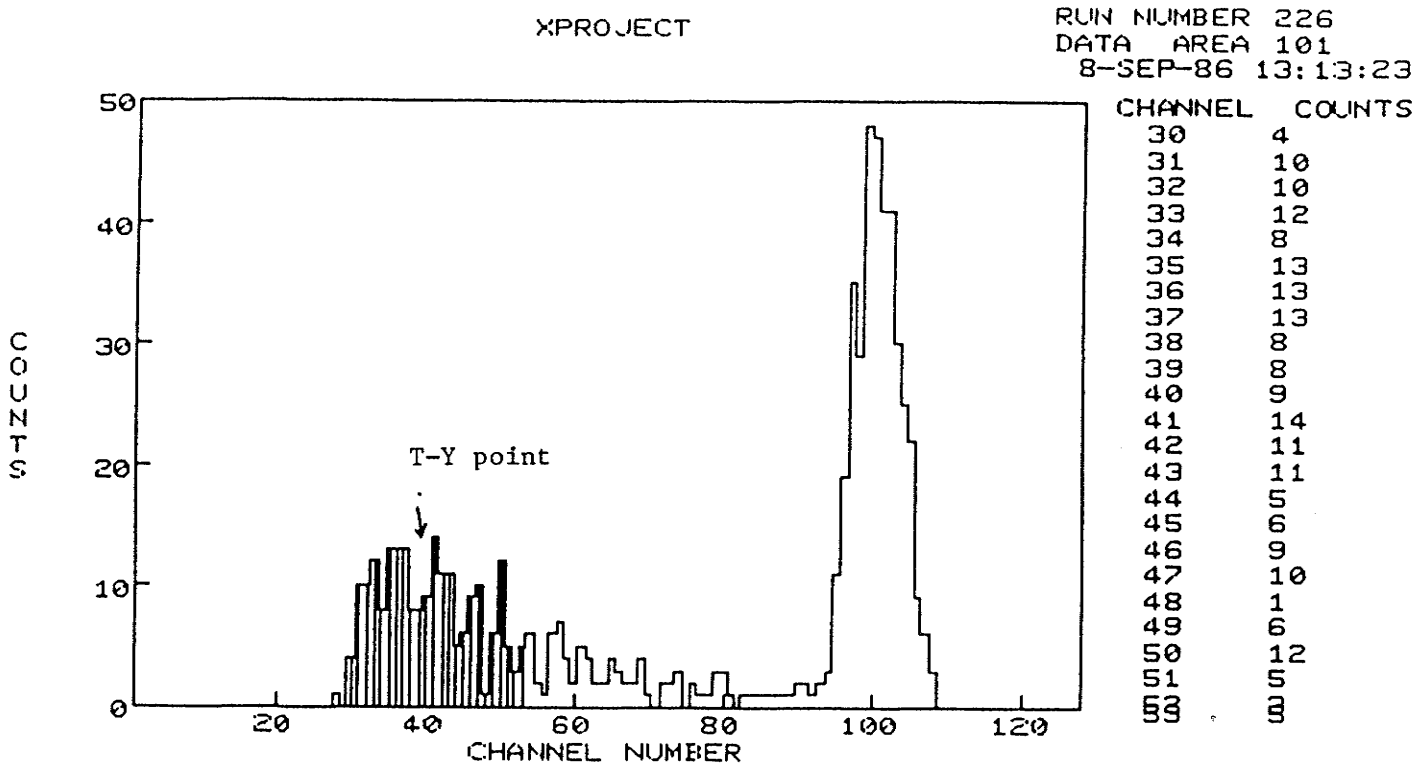

fig (4.6.5)Projection onto E axis of proton-deuteron breakup spectra

(Treiman-Yang angle $\varepsilon = 90^{\circ}$)

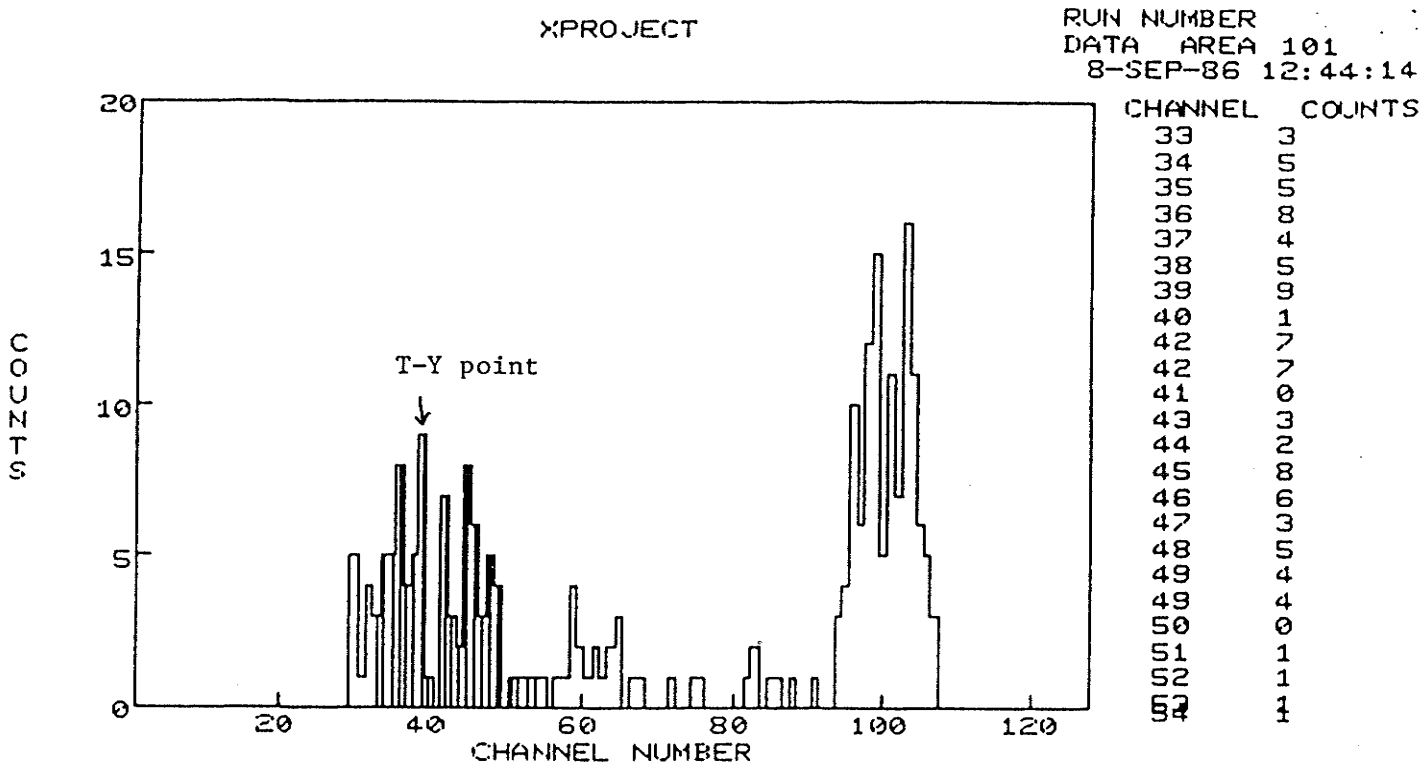

fig (4.6.6) Projection onto E axis of proton-deuteron breakup spectra

(Treiman-Yang angle $\epsilon = 110^{o}$)

4.7 CROSS SECTION CALCULATIONS

Once a printout of the in-plane versus out-of-plane energy spectrum is available one may readily calculate the breakup cross section from the formula

$$N_i = \frac{d^3\sigma}{d\Omega_3 d\Omega_4 dE_4} \; d\Omega_3 x d\Omega_4 x dE_4 x t \; (\text{nucl/cm}^2) x \; N_p$$

where

$d\Omega_3$ is the solid angle of the in-plane counter telescope,

$d\Omega_4$ is the solid angle of the out-of-plane counter telescope.

N_p is the number of protons that pass through the target and is equal to the charge deposited by the beam current in coulombs divided by the proton charge in coulombs; t is the thickness of the target in nucl/cm^2; N_i is the number of counts in each projected channel; dE is the channels |MeV.

The formula applies to the case where the in-plane versus out-of-plane locus has been projected onto the y-axis. The incoming data were collected with a full resolution of 1024 channels but the projected spectra were condensed to 64 channels.

CHAPTER FIVE

Results and Conclusion

Measurements have been made at the seven combinations of angles shown in table (5.1) the in-plane detector telescope was kept at the fixed position $\theta_1 = 15°$ and $\phi_1 = 0°$. The results after particle identification and background subtraction are shown in figure (5.1) projected onto the fixed detector energy axis. The error bars include counting statistics and uncertainties due to background subtraction.

This part of the data for a value $E_1 = 4.2$ MeV in the fixed detector counts are integrated over five channels around the Treiman-Yang point. The data were analysed by assigning each event to a Treiman-Yang angle and a spectator momentum q. The resulting Treiman-Yang distribution is shown in figure (5.1) were compared with "exact" three-body calculations by J.P. Svenne using the Doleschall three-body code.

The data from the experiment are in good agreement with theoretical calculations at the Treiman-Yang point under the kinematic situation of a Treiman-Yang cone.

Calculated cross sections from the experiment and from theoretical calculations are shown in table (5.2).

In conclusion, theoretical prediction and calculations made by J.P. Svenne indicates excellent agreement with the results of the experiment.

Also, our complete measurement of the Treiman-Yang distribution shows that at 11.2 MeV energy the pole graph does not give a sufficient description of kinematics of the mechanism of the reaction and the Treiman-Yang test is not satisfied for the conditions chosen in this experiment.

It is clear that Treiman-Yang criterion is not fulfilled for p+d reaction at 11.2 MeV bombarding energy for the conditions studied in this work because of the nucleon momentum transfer is not small which indicates that strong contribution or interference effects from other graphs must be present in this reaction even under conditions seemingly favourable for contributions for one pole graph only.

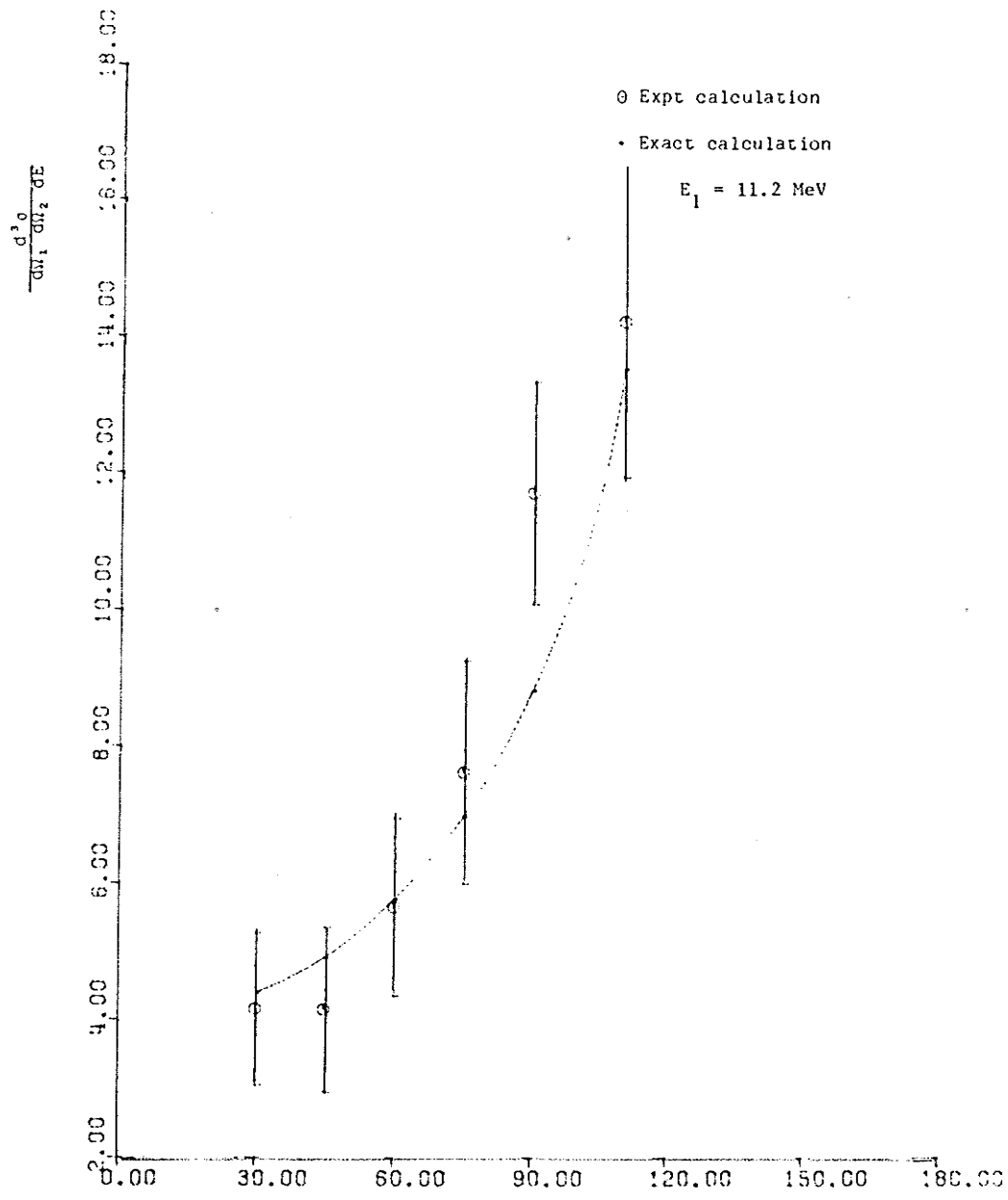
0 Expt calculation
• Exact calculation
E_1 = 11.2 MeV
$\frac{d^3\sigma}{d\Omega_1 d\Omega_2 dE}$
2.00
4.00
6.00
8.00
10.00
12.00
14.00
16.00
18.00
0.00
30.00
60.00
90.00
120.00
150.00
180.00
Treiman-Yang angle

fig (5.1)

ε (deg)	θ_1 (deg)	ϕ_1 (deg)	θ_2 (deg)	ϕ_2 (deg)
0	15	180	36	0
30	15	180	34.7	12.93
45	15	180	33.27	19.215
60	15	180	31.218	25.255
75	15	180	28.661	30.947
90	15	180	25.66	36.134
110	15	180	21.097	41.806

Table (5.1)

ε (deg)	Cross Section(mb/sr²/MeV)	
	Theoretical	Experimental
30	4.39	4.2 ± 1.1
45	4.90	4.2 ± 1.2
60	5.76	5.7 ± 1.3
75	6.97	7.6 ± 1.6
90	8.8	11.7 ± 1.6
110	13.5	14.2 ± 2.3

Table (5.2)

REFERENCES

1. I.S. Shapiro, In 'Interactions of high-energy particles with nuclei', Proceeding of the International School of Physics "Enrico Fermi" Course 38, edited by T.E. Ericson (Acadamic, New York, 1967), p. 232.

2. I.S. Shapiro, V.M. Kolybasov, and G.R. August, Nucl. Phys. 61, 353 (1965).

3. S.B. Treiman and C.N. Yang, Phys. Rev. Lett. 8, 140 (1962).

4. L.C. Biedenharn, K. Boyer, and R.A. Charpie, Phys. Rev. 88, 517 (1952).

5. V.M. Kolybasov, Yad. F12 5, 288 (1967) [Sov. J. Nucl. Phys. 5, 202 (1967)].

6. G.F. Chew and F.E. Low, Phys. Rev. 113, 1640 (1959).

7. A.F. Kuckes, R. Wilson, and P.F. Cooper, Jr. Ann. Phys.(New York) 15, 193 (1961).

8. R. Corfu et al., Phys. Rev. Lett. 27, 24 (1971) 1661.

9. R. Corfu et al., Helv. Phys. Acta 43 (1970) 443.

10. A.O. Aganyants et al., Nucl. Phys. B.11 (1969) 79.

11. Y.D. Bayukov et al., Phys. Lett. 33B (1970) 416.

12. A.D. Ijpenberg et al., Few-Particle Problems in the Nuclear Interaction, ed. I. Slaus et al., (North Holland, Amsterdam 1972) p. 651.

13. N.T. Okumusoglu et al., Nucl. Phys. A.231 (1974) 391-396.

14. A. Moussa, J. Birchall, J.S.C. McKee, University of Manitoba Cyclotron Lab. Annual Report (1984-85) 102.

15. M.H. MacGregor, R.A. Arndt and R.M. Wright, Phys. Rev. 122, 1710 (1969).

16. A. Johansson et al., Uppsala, Sweden 'Few Particle Problems in the Nuclear Interaction', edited by I. Slaus et al., p. 491.

17. A. Valkovic. Nucl. Phys. A 166 (1971) 547.

18. D.J. Margaziotis et al., Phys. Rev. C2 (1970) 2050.

19. W. Ebenhöh, Habilitationschrift Universität Heidelberg, 1971.

20. J.P. Didelez, "Few Particle Problems in the Nuclear Interaction" edited by Ivo Slaus, Steven A. Moszkowski, Roy P. Haddock, W.T.H. van Oers, p. 384.

21. K. Kuroda et al., Proc. Int. Conf. Nucl. Stuct. Tokyo (1967) 76.

22. F. Takeuchi et al., Nucl. Phys. A152 (1970) 434.

23. E.L. Petersen et al., U.S. Naval Research Lab., Washington, D.C., 'Few Body Problems in the Nuclear Interaction', edited by I. Slaus et al., p.503.

24. E.L. Petersen et al., Phys. Rev. 188 (1969) 1497.

25. E.L. Petersen et al., Phys. Lett. 31B (1970) 209.

26. J. Birchall, J.P. Svenne, J.S.C. McKee, Phys. Rev. C 20 (1979) 1585.

27. P. Doleschall, Nucl. Phys. A 220, 491 (1974).

28. W. Ebenhöh, Nucl. Phys. A. 191, 97 (1972).

29. E.L. Petersen and J.M. Wallace, Phys. Rev C 14, 419 (1976).

30. J.J. Benayoun et al., Phys. Rev. Lett. 36, 1438 (1976).

31. J. Bruinsma and R. van Wageningen, Nucl. Phys. A 282 1 (1977).

32. B. Sundqvist, in Few Body systems and nuclear forces II Lecture notes in physics, edited by H. Zingl et. al., (Springer, Berlin, 1978) v. 87, p. 295.

33. K.G. Standing, J.J. Burgerjon and F. Konopasek, Nucl. Intr. and Meth. 18, 111 (1962).

34. J.J. Burgerjon, F. Konopasek and K.G. Standing, IEEE Trans. on Nucl. Sci., NS-12, 334 (1965).

35. J.J. Burgerjon, B. Hird, F. Konopasek and K.G. Standing, IEEE Trans. on Nucl. Sci., NS-13, 422 (1966).

36. D.J. Clark, R.R. Richardson and B.T. Wright, Nucl. Instr. and Meth 18, 1 (1962).

37. M.E. Rickey and R. Smythe, Nucl. Instr. and Meth. 18, 66 (1962).

38. A.C. Paul and B.T. Wright, IEEE Trans. on Nucl. Sci., NS-13, 74 (1966).

39. C.J. Kost Ph.D. Thesis, University of Manitoba, 1968.

40. B.M. Bardin and M.E. Rickey, Rev. Sci. Instru. 35, 962 (1964).

41. R. Smythe, Rev. Sci. Instr. 35, 1197 (1964).

42. McDonald, A.M., Studies of the Non-coplanar $\vec{H}(p,2p)n$ Reaction and Faddeev type S-wave model theoretical predictions, Ph.D. Thesis, University of Manitoba, 1976.

43. E.J. Burge and D.A. Smith, Rev. Sci. Instr. 33, 1371 (1962).

44. F.G. Resmini, A.D. Bacher, D.J. Clark, E.A. McClatchie and R. de Swiniarski, Nucl. Instr. and Meth. 74, 261 (1969).

45. C.M. Bartle, Nucl. Instr. and Meth. 144 (1977) 599.

46. C.M. Bartle and H.O. Meyer, Nucl. Instr. and Meth. 112 (973) 615.

47. I.J.R. Aitchison and C. Kascer, Phys. Rev. 142, 1104 (1966).

48. R. Fox, Phys. Rev. 125, 311 (1962).

49. L.D. Faddeev, Zh. Eks. Teor Fiz. 39, 1459 (1960) [Sov. Phys. - JETP 12, 1014 (1961)].

50. P. Doleschall, Nucl. Phys. A201, 264 (1973).

51. C. Lovelace, Phys. Rev. 135, B1225 (1969).

52. J.P. Svenne, J. Birchall and J.S.C. McKee, Phys. lett 119B, 269 (1982).

53. E.O. Alt, P. Grassberger and W. Sandhas Nucl. Phys. B2 (1967) 167.